Vibrational levels of formaldehyde: Calculations from new high precision potential energy surfaces and comparison with experimental band origins

Andrei V Nikitin, Alexander E Protasevich, Alena A Rodina, Michael Rey, Attila Tajti, Vladimir G. Tyuterev

Vibrational levels of formaldehyde: calculations from new high precision potential energy surfaces and comparison with experimental band origins

Andrei V. Nikitin[1], Alexander E. Protasevich[1], Alena A. Rodina[1], Michael Rey[2], Attila Tajti [3], and Vladimir G. Tyuterev[2,4]

[1.] *V.E. Zuev Institute of Atmospheric Optics, Russian Academy of Sciences, 1, Akademichesky Avenue, 634055 Tomsk, Russian Federation*
[2.] *Groupe de Spectrométrie Moléculaire et Atmosphérique, UMR CNRS 6089, Université de Reims, U.F.R. Sciences, B.P. 1039, 51687 Reims Cedex 2, France*
[3.] *ELTE Eötvös Loránd University, Institute of Chemistry, Laboratory of Theoretical Chemistry, P. O. Box 32, H-1518, Budapest 112, Hungary*
[4] *QUAMER, Tomsk State University, 36 Lenin Avenue, 634050 Tomsk, Russian Federation*

Number of Pages: 27
Number of Figures: 8
Number of Tables: 9
Number supplemental files: 1

Running Head: Vibration energy levels of formaldehyde

Keywords: formaldehyde, potential energy surface, vibrational energy levels, kinetic energy operator

Correspondence should be addressed to:
Andrei V. Nikitin,
*Laboratory of Theoretical Spectroscopy, V.E. Zuev Institute of Atmospheric Optics, SB RAS, 1, Academician Zuev square, 634021, Tomsk, Russia
E-mail: avn@iao.ru
Phone : +73822 – 491111 (ext. 1208)

Abstract

Vibrational energy levels of H_2CO are reported using ~~global~~ variational nuclear motion calculations from new ab initio and empirically optimized full 6-dimensional ab initio potential energy surfaces in ground electronic state of the formaldehyde molecule. Ab initio calculations were carried out using extended electronic structure coupled-cluster calculations accounting for dynamic electron correlations including triple and quadruple excitations as well as relativistic and diagonal Born-Oppenheimer corrections. Variational nuclear motion calculations are compared in different set of coordinates with exact kinetic energy operator and in normal coordinates with Watson-Eckart kinetic energy operator. Our best ab initio potential energy surface including the above mentioned contributions provides the RMS (obs.-calc.) errors of 0.25 cm^{-1} for fifteen vibrational band centers without empirically adjusted parameters. The average error drops down to 0.08 cm^{-1} for an empirically optimized potential energy function with six adjusted parameters corresponding to quadratic force field terms. The estimation of the accuracy for the calculated vibrational levels in an extended range up to 4500 cm^{-1} shows that the set of ab initio vibrational levels could be more consistent than experimental levels obtained from earlier studies of low resolution spectra. The comparison of the calculated and experimental vibrational energy levels of the D_2CO isotopologue is also reported.

1. Introduction

Accurate knowledge of spectroscopy of formaldehyde is important for the monitoring of this species in the atmosphere and also for detection of the presence of this molecule as an environmental pollutant indoors [**1**] [**2**] [**3**] [**4**]. Improving spectral parameters and line-by-line analyses are essential for reliable interpretation of near infrared spectra returned by the ground-based and orbiting observatories [**5**] [**6**]. An assignment of infrared spectra corresponding to high-energy overtone and combination bands is known to be a tedious and difficult task. Recent ab initio calculations of potential energy surfaces (PES) and of dipole moment surfaces (DMS) together with a progress in variational nuclear motion calculation have permitted a significant progress in predictions of vibration-rotation bands. Previous experience with some 4-5 atomic molecules [**7**] [**8**] [**9**] [**10**] [**11**] have shown that ab initio based approaches could be useful for better modelling and assignments of high-resolution spectra. In the present work, we report theoretical vibrational levels of formaldehyde computed from new accurate ab initio PES using the algorithms similar to one recently applied for the methane molecule [**12**] and compare our results with other recent calculations [**13**] [**14**].

From the theoretical standpoint, the formaldehyde molecule is an interesting case because of the rapid basis set convergence of variational calculations and a possibility to compare different

methods conducted in various coordinate systems using high-level quantum-chemical calculations. Burleigh et al. [**15**] have been used the quadratic force field for formaldehyde obtained by refining the *ab initio* quartic force field CCST(T)/cc-pVTZ of Martin, Lee, and Taylor [**16**] by means of iteratively fitting a subset of the coefficients of a Taylor-series expansion of the potential-energy surface to the set of the observed transition frequencies. Yachmenev et al. [**14**] have calculated ab initio PES using CCSD (T) / aug-cc-pVQZ method in a wide range of geometries. A detailed review of earlier works refs [**17**] [**15**] [**16**] [**18**] [**19**] [**20**] that reported calculations of the formaldehyde PES and energy levels can be found refs. [**13**] [**14**].

The accuracy of ab initio calculations is in general lower than that of high-resolution experimental methods, except for studies of diatomic molecules with a small number of electrons. In the case of triatomics, very accurate ab initio calculations of potential energy surfaces (PES) and of dipole moment surfaces (DMS) led to a breakthrough in the extension of spectra analyses towards higher energy ranges. This was, for example, the case with the spectroscopy of water [**21**] [**22**] [**23**] [**24**], carbon dioxide [**25**] [**26**] [**27**], hydrogen sulfide [**28**] [**29**] and sulfur dioxide [**30**], as well as with the ozone spectra analyses [**31**] [**32**] [**33**]. In the latter case, ab initio predictions were mandatory for precise intensity quantification [**34**], for understanding the PES properties in the transition state range towards the dissociation threshold [**35**] [**33**], the interactions between potential wells [**36**], and modeling of the isotopic exchange reactions [**37**]. Many ab initio PESs have been subsequently refined by a fit to experimental data to achieve better accuracy in line positions. Theoretical line lists for ammonia [**38**] [**27**] and phosphine [**39**] [**40**] [**41**] are successful examples of this trend for four-atom species. New PESs and DMSs have been recently reported for five-atom [**42**] [**43**], six-atom molecules [**44**] [**45**], [**46**] and seven-atom [**47**] molecules.

Among the large number of ab initio calculations for many-electron systems, only two works reported calculations of the vibrational levels with the accuracy of about 0.1 cm^{-1}, at least in the low and medium energy ranges: ref [**24**] [**48**] for the water molecule, and ref [**12**] for methane. While both of these molecules contain 10 electrons, the formaldehyde molecule has 16 electrons. In the recent study by Morgan et al. [**13**] the high accuracy vibrational fundamentals of formaldehyde have been reported, but not all calculated vibrational energy levels were published.

In contrast to methane, formaldehyde is an experimentally much less studied molecule. One of the possible reasons for this is the unavailability of the cold spectra caused by the high temperature of congelation and a complex technique for creating the formaldehyde gas. While

for methane about 200 assigned vibrational energy levels have been measured with high accuracy, in case of formaldehyde, no more than 20 vibrational levels could be accurately obtained from the high resolution rotationally resolved spectra. The calculations reported in this paper can be considered as an additional source of information that could be useful for extended assignment and modeling of high-resolution experimental spectra of formaldehyde and its isotopologues.

This paper is structured as follows. The choice of the coordinates, the kinetic energy operator (KEO) and the analytical representations for the PES including their benchmark comparisons are discussed in Section 2. The dependence of the theoretical vibrational levels on the electronic basis set, the impact of relativistic corrections, diagonal Born-Oppenheimer corrections (DBOC), and of high-order electron correlation including connected triple and quadruple excitations in the coupled-cluster method is considered in Section 3. A detailed comparison with available experimental data in Sections 3 and 4 shows that the resulting full-dimensional ab initio PES provides currently the most accurate theoretical band origins for formaldehyde. We also discuss uncertainties and discrepancies in published experimental levels obtained from low- and high-resolution spectra. An empirically optimized PES obtained with a fine tuning of six PES parameters and the corresponding predicted vibrational levels are also reported.

2. Coordinates and analytical PES representation

For calculations of the vibrational-rotational energy levels of the formaldehyde molecule we used the kinetic energy operator (KEO) and PES written in terms of three sets of internal coordinates based on the angle-bisector molecule fixed axes [**49**], [**50**] . The sets of coordinates differ only in the definition of the internal vectors: (I) bond angle-bond length coordinates in which KEO was derived in ref [**50**], (II) Jacobi-like coordinates (see later), (III) Radau–Jacobi coordinates from refs [**51**] and [**52**]. The internal coordinates (I) and (II) are non-orthogonal sets while (III) is an orthogonal coordinate set. The kinetic energy operator of the nuclei (using the notation from ref [**53**]) in the laboratory frame

$$\hat{T}_L = -\frac{1}{2}\hbar^2 \sum_{k=1}^{4} \frac{1}{m_k} \frac{\partial^2}{\partial \vec{R}_k^2}$$

can be written as a sum of the KEO of the center of mass and the T_R relative motions of the nuclei~~, as follows~~:

$$\hat{T}_R = -\frac{1}{2}\hbar^2 \sum_{i=1}^{3}\sum_{j=1}^{3} \frac{1}{m_{i,j}} \frac{\partial^2}{\partial \vec{r}_i \partial \vec{r}_j},$$

where the effective masses are given by

$$\frac{1}{m_{i,j}} = \sum_{k=1}^{4} \frac{A_{ik}A_{jk}}{m_k},$$

where m_k is the mass of the k[th] nuclei, and the linear transformation of the 4 original nuclear position vectors $\vec{R}_k$ to new 3 internal vectors $\vec{r}_i$ is defined as follows:

$$\vec{r}_i = \sum_{k=1}^{4} A_{ik}\vec{R}_k \ . \qquad (1)$$

Let us use the following numbering of indices: 1- for the nucleus of the first hydrogen atom H_1, 2 – for the nucleus of the second hydrogen atom H_2, 3 – for oxygen O, 4 – for carbon C. The vectors $\vec{R}_1$, $\vec{R}_2$, $\vec{R}_3$, and $\vec{R}_4$ start from the same point and define the positions of the H_1, H_2, O, and C nuclei, respectively. m_1, m_2, m_3, and m_4 are masses of the H_1, H_2, O, and C nuclei, respectively. New vectors (1) $\vec{r}_1$, $\vec{r}_2$, and $\vec{r}_3$ define the relative positions of the H_1, H_2, and O nuclei with respect to different centers of mass. The differences in the coordinate systems are as follows: for (I), $\vec{r}_1$, $\vec{r}_2$, and $\vec{r}_3$ start from the C nucleus position; for (II), $\vec{r}_1$, $\vec{r}_2$, and $\vec{r}_3$ start from the CH_1H_2 center of mass; for (III), $\vec{r}_1$ and $\vec{r}_2$ start from the Radau canonical point for the CH_1H_2 group, and $\vec{r}_3$ starts from the CH_1H_2 center of mass. Figure 1 shows these three sets of the internal vectors. Table 1 gives the matrix elements $\|A_{ik}\|$ and values of $1/m_{i,j}$ for these coordinate sets.

Table 1. Elements of the matrix of transformation to internal vectors and the effective masses for three sets of coordinates.

Set of coordinates	A_{ik}	$1/m_{i,j}$
(I)	$\delta_{ik} - \delta_{4k}$	$\frac{1}{m_i}\delta_{ij} + \frac{1}{m_4}$
(II)	$\delta_{ik} + \frac{m_k}{m_1 + m_2 + m_4}(\delta_{3k} - 1)$	$\frac{1}{m_i}\delta_{ij} + \frac{1}{m_1 + m_2 + m_4}(\delta_{3i} + \delta_{3j} - 1)$

(III)	$\delta_{ik}+\delta_{3i}\dfrac{m_k}{m_1+m_2+m_4}(\delta_{3k}-1)+$ $(1-\delta_{3i})\left((\delta_{3k}+\delta_{4k}-1)\dfrac{m_k}{m_1+m_2}(1-\alpha)-\delta_{4k}\alpha\right)$ [a]	$\dfrac{1}{m_i}\delta_{ij}+\dfrac{1}{m_1+m_2+m_4}\delta_{3i}\delta_{ij}$

154 [a] the parameter $\alpha=\sqrt{m_4/(m_1+m_2+m_4)}$.

155

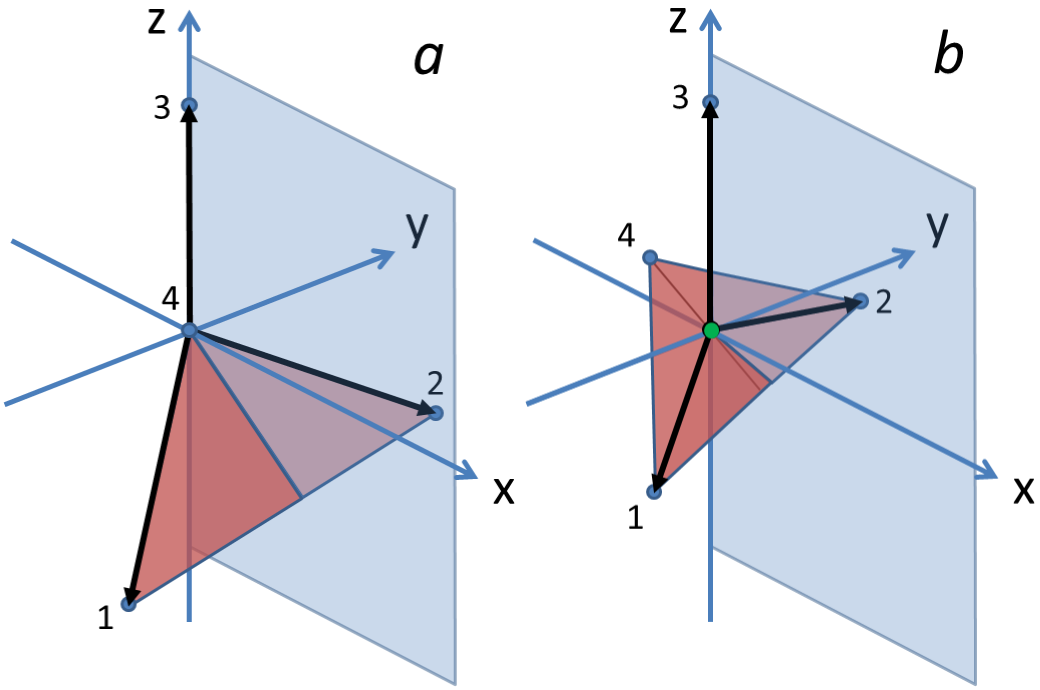

156

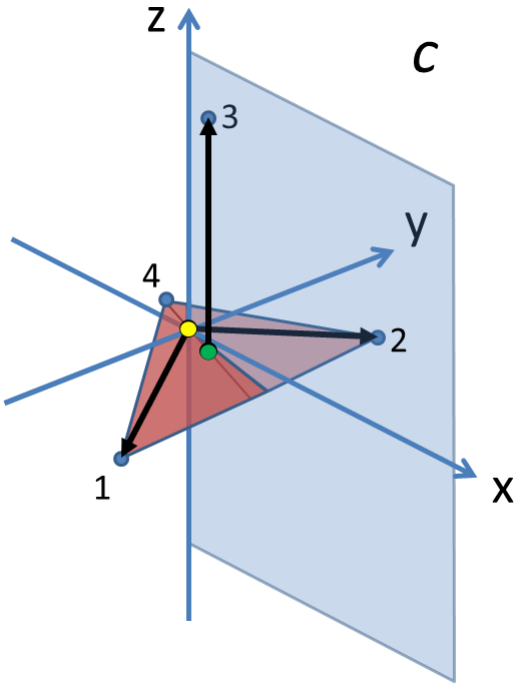

157

Figure 1. Internal vectors (depicted in black) for three sets of the internal coordinates based on the angle bisector coordinate system for the the formaldehyde molecule : *a*) bond angle-bond length coordinates (I), *b*) Jacobi-like coordinates (II), *c*) Radau–Jacobi coordinates (III). The 1, 2, 3, and 4 indices denote the H_1, H_2, O, and C atom nuclei, respectively. Internal vectors with heads in the positions of nuclei 1, 2, and 3 have the following starting point: *a*) in the position of the nucleus 4, *b*) in the center of mass of the nuclei 1, 2, and 4 (depicted in green) *c*) in the canonical point (depicted in yellow) of the nuclei 1, 2, and 4 (for vectors with heads in 1 and 2), and in the center of mass (depicted in green) of the nuclei 1, 2, and 4 (for the vector with head in 3).

Here we applied the same tensor techniques for an optimal sampling of the grid of nuclear configurations as described in the previous works for non-abelian symmetry groups [**54**] [**55**]. This permitted accounting for the full symmetry of the molecule in order to reduce the number of geometrical nuclear configurations for ab initio calculations of electronic energies. To build the corresponding grid of geometries, we used at the first step six one-dimensional sections(Figure 2 show three angular sections). The extent of the grid points was chosen in a way which ensures that a maximum number of parameters of our analytical PES representation would be well-defined in the least-squares fits to ab initio electronic energies. PES parameters responsible for the coupling of various vibrational modes were systematically included. The corresponding initial reference grid ($G^{(R)}$) contained 22509 points. This relatively dense grid provides a possibility for testing various high-order PES expansions in elementary functions of the symmetrized coordinates. The grid points were arranged in the order of increasing energy with the cut-off corresponding to the extent of the studied infrared bands. For this grid, the initial calculations were carried out with the coupled-cluster CCSD(T) method using the frozen core approximation and the quintuple-zeta cc-pV5Z basis set (that will be referred to as V5Z sets in abbreviated notation) and the MOLPRO program [**56**] [**57**].

The analytical PES was constructed using the irreducible tensor formulation described in refs [**54**] [**55**]. The PES can be expressed as a power series in elementary functions of the symmetrized coordinates involving Morse-type functions for “radial” and a sine function of angular variables:

$$V(r_1, r_{CO}, r_2, \theta_1, \theta_2, \tau) = \sum_{ijklmn} f_{ijklmn} S_1^i S_2^j S_3^k S_4^l S_5^m S_6^n \text{, where} \qquad (2a)$$

$$S_1 = \left(y(r_1) + y(r_2)\right)/\sqrt{2}, \quad S_2 = y(r_{CO}), \quad S_5 = \left(y(r_1) - y(r_2)\right)/\sqrt{2}, \qquad (2b)$$

$$S_3 = \left(f(\theta_1) + f(\theta_2)\right)/\sqrt{2}, \quad S_6 = \left(f(\theta_1) - f(\theta_2)\right)/\sqrt{2}, \quad f(\theta) = \sin(\theta - \theta_e). \qquad (2c)$$

A Morse-type function $y(r) = 1 - \exp(-a(r - r_e))$ with the parameter $a=1.9$ is used as radial function. For the angles between bonds, the elementary function for the expansion is chosen as

$f(\theta) = \sin(\theta - \theta_e)$. Note that the angular fitting that uses the function $f(\theta) = \sin((2/3)(\theta - \theta_e))$ improves the accuracy of the fit to a minor extent. However, we did not use this function because it requires the numerical evaluation of one-dimensional integrals. The torsion angle τ is the angle between two planes $\vec{r}_1 \times \vec{r}_3$ and $\vec{r}_2 \times \vec{r}_3$. The following functions: $\cos(\tau)+1$, $\cos(\tau/2)$, $\tau - \pi$ have been tested as the torsion function $S_4(\tau)$. The first function transforms as the A_1 irreducible representation while the second and third functions transform as B_1. Contrary to the case of methane [**12**] [**55**], the expansion (2) does not contain components of degenerate vibrations due to the simplicity of the Abelian C_{2v} point group.

To validate various representations of the PES using the least-squares technique, an extended grid of geometries was used. This grid was augmented by adding supplementary sets of points corresponding to 180-τ values with respect to all values of τ (for $\tau \neq 180$) in the initial grid.

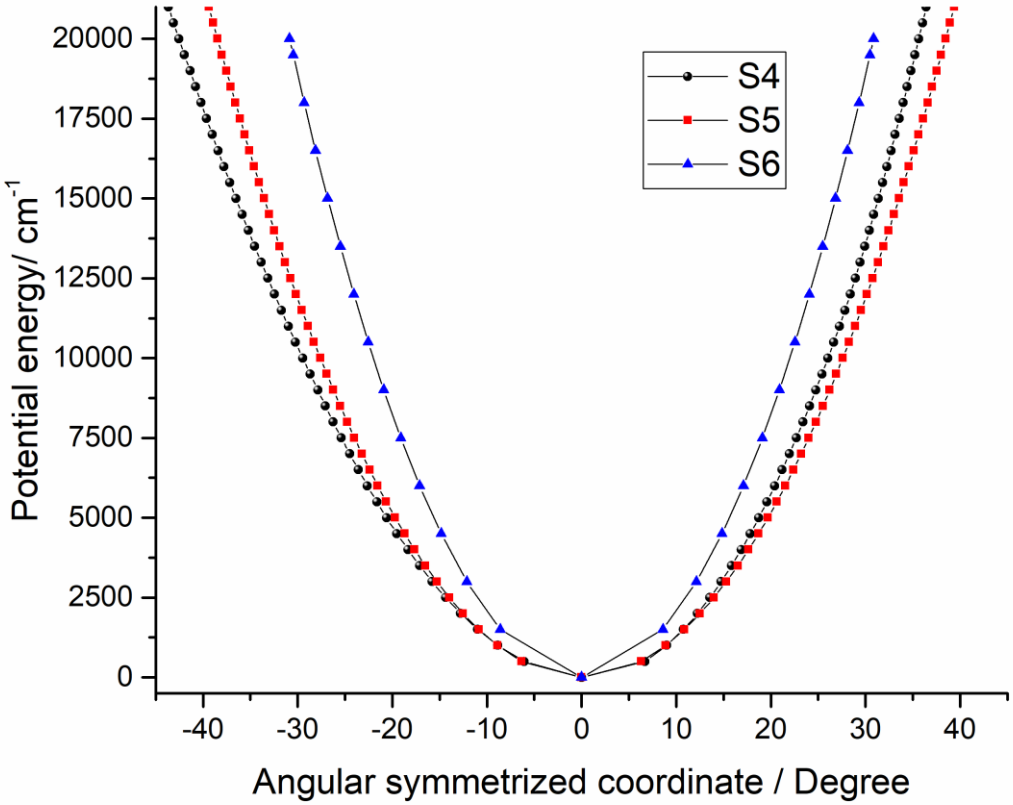

Figure 2. One-dimensional PES sections for angular symmetrized coordinates.

To compare the efficiency of the analytical form (2) in various coordinate sets, the benchmark PES calculations were carried out using the least-squares fit to V5Z grid values,

without the further corrections discussed in the following sections. Even though the V5Z basis set did not provide the best quantitative accuracy, we considered that it was preferable to use all PESs at the same theoretical level without corrections for a reliable comparison of the general qualitative shape of the surfaces. A*b initio* potential energies were fitted using the analytical symmetry adapted representation (3) and the weight function employed by Schwenke and Partridge in ref [**58**]

$$w(E) = \frac{\tanh(-0.0005(E - E_1) + 1.002002002)}{2.002002002}. \quad (3)$$

This weight function decreases with the energy E (expressed in cm^{-1}) in order to de-emphasize the contribution to the PES fit of large grid displacements for vibrational energies beyond E_1=15000cm^{-1}. The least-squares fit of the PES in various sets of coordinates leads to quite similar results, but for the coordinate sets II and III, the RMS deviations slightly decrease at $E_1 >$ *12000* cm^{-1}. Table 2 summarizes the RMS deviations of the fit in various coordinates. The PES expansion was extended up to sixth order in all S_i-coordinates including the torsion function cos(τ)+1 but some eighth-order terms were added for torsion functions cos(τ /2) and τ-π.

The number of parameters, which were statistically well determined in the fit of the PES to ab initio electronic energies, versus the total number of parameters of the corresponding expansion orders, is given in the second row of Table 2. The results show that the coordinate sets (II) and (III) provide a more accurate description of the PES when using the weight function (3). When fitting a six-dimensional PES, all three forms of the torsion function result in close lying standard deviation (STD) values but the use of (II) and (III) provides slightly lower RMS values. Ref [**14**] reported a more complicated PES representation, but the use of that representation was not found useful in our case.

Table 2. RMS and standard deviations of the PES fits in various coordinate sets.

Coordinates PES, #Calc,	(I) Internal Fig. 1 (a), Calc 1	(I) Internal Fig. 1 (a), Calc 0	(I) Internal Fig. 1 (a), Calc 4	(II) O-X X(CH_1H_2) Fig. 1 (b), Calc 2	(III) Orthogonal Fig. 1 (c), Calc 3
Torsion function	cos(τ)+1	cos(τ /2)	τ -π	cos(τ/2)	cos(τ/2)
#Parameters/ Initial # Param	342/502	344/576	338/576	358/576	356/576
KEO	Exact	Exact	Watson	Exact	Exact
RMS (STD)	1.58 (1.25)	1.99(1.27)	1.59(1.24)	1.09(0.84)	1.14(0.84)

Note: Abbreviation KEO stands for kinetic energy operator

To control the equilibrium geometry, we calculated the rotational energy levels combining the V5Z PES with the equilibrium geometries optimized using larger basis sets. This corresponds to a series of calculations using the aug-cc-pCVXZ core-valence basis sets augmented with diffuse functions for one-particle basis cardinal numbers X = 4 and 5 (denoted simply as ACVQZ, and ACV5Z). We have also accounted for the Douglas-Kroll (DK) type relativistic corrections. The parameters of the equilibrium geometry affect the vibrational energy levels, especially those associated with the angular motions [**55**]. Table 3 gives the equilibrium geometry parameters, while Table 4 gives the energy levels at J=1 for the equilibrium geometries mentioned in Table 3. Note that changes up to the fourth decimal place do not affect the vibrational energy levels. That is why, the calculations for all geometries except for the first one, led to almost identical results for the low lying rotational levels. The accuracy of the known experimental rotational levels was estimated to be about 10^{-4} cm^{-1}. In this work, however, we did not have an intention to obtain highly accurate values of the rotational levels, but to find the appropriate parameters of the equilibrium geometry consistent with reliable vibrational predictions.

Table 3. Equilibrium geometry of the formaldehyde molecule, as optimized at various levels of ab initio theory

Coordinates	CCSD(T)/ ACVQZ	CCSD(T)/ ACV5Z	CCSD(T)-DK/ ACV5Z-DK**	Morgan [**13**]	Empirical values [**59**] [**60**]
r_e(CO) / Å	1.205240	1.20437	1.20426	1.20457	1.20461(19)
r_e(CH) / Å	1.100744	1.10041	1.10031	1.10052	1.10046(16)
θ(HCH) / Deg	116.6186	116.6495	116.6546	116.694	116.722(93)
θ(OCH)* / Deg	121.6906	121.6752	121.6726	121.653	121.639

* θ(OCH)=π- θ(HCH)/2
** accounting for Douglas-Kroll-Hess relativistic corrections

Table 4. The energy levels (in cm^{-1}) obtained for the equilibrium geometries from Table 3 with the (V5Z) PES.

J=1 Levels	Exp.*	ACV5Z** Watson KEO	ACV5Z** "Exact" KEO	Morgan [**13**]	Empirical values [**59**] [**60**]
A_2	2.4295	2.422452	2.426531	2.421981	2.422041
B_1	10.5395	10.539508	10.537128	10.533067	10.531232

B_2	10.7006	10.699928	10.702374	10.693525	10.691728

* Experimental values [**61**] [**60**].
** Basis sets used for the equilibrium geometry. KEO stands for the kinetic energy operator used in the calculations

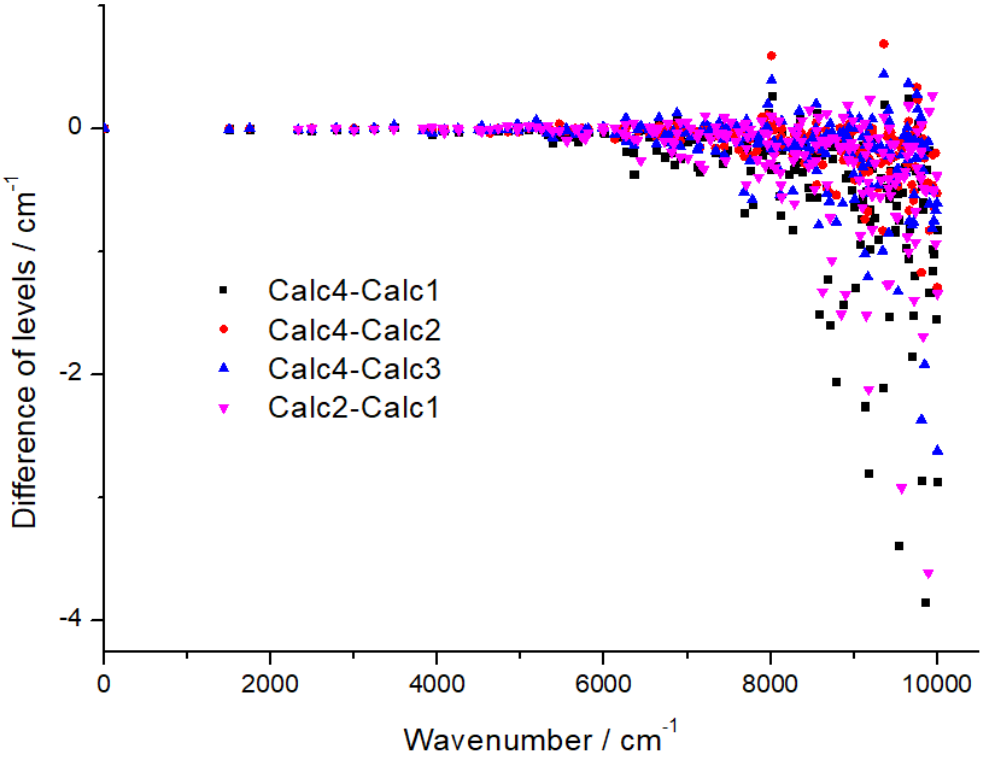

Figure 3. Comparison of the energy levels (the symmetry block A_1) for four calculations. The variational methods and the ab initio PES versions corresponding to Calc1, Calc2, Calc3 and Calc4 are defined in Table 2.

Figure 3 displays the diagram of differences in the calculated levels for the symmetry block A_1. The diagram shows that the difference between the fourth and the first calculation is considerable in the range over 8000 cm^{-1}. This is mainly caused by the different torsion parts. Below 7000 cm^{-1}, all calculations lead to close results. Below 4500 cm^{-1}, the influence of the PES type on the energy levels is not significant: the differences in the level positions do not exceed 0.05 cm^{-1}.

3. Improvement of the basis set and corrections to the PES

Since all versions of calculations for levels up to 7000 cm^{-1} using the V5Z basis in the previous sections lead to close results, we shall use the internal coordinate set (I) and torsion function $\cos(\tau/2)$ while improving the PES at higher levels of the theory. The choice of the shape is due to the fact that the internal coordinates are easier for calculating corrections.

First of all, we conducted calculations according to the procedure described for the methane molecule in ref [**12**] using the augmented core-valence basis set ACV5Z at a sparser grid of

geometries. As these calculations are more demanding, we computed electronic energies with the CCSD(T)/ACV5Z level of theory at the grid ($G^{(AC)}$) containing only 3820 points in the range up to about 6000 cm^{-1} from the equilibrium geometry. Similarly to ref [**12**], the energy differences Δ_{AC}= ACV5Z-V5Z involving two basis sets were computed on this grid. We have checked that these differences behave quite smoothly with respect to the symmetrized coordinates S_i and were possible to be modeled analytically using the fourth-order expansions Δ_{AC} (S_i) of the type (2a-2c). This allowed us to extend the electronic energies according to the relation ACV5Z ≈V5Z + Δ_{AC} (S_i) for all remaining geometries and refitting the PES(ACV5Z) on the full reference grid $G^{(R)}$ of 22509 points using the analytical form (2a) as discussed in the previous section.

As the next step, we accounted for the following *three corrections* to the surface: "mass-velocity-Darwin" (MVD) relativistic corrections, the diagonal Born-Oppenheimer correction (DBOC), and higher-order dynamic electron correlations (HODEC). The adiabatic DBOC corrections [**62**] [**63**] [**64**] [**65**] [**66**], which are the leading first-order contributions to the electronic energy beyond the Born-Oppenheimer approximation have been included in accurate PES calculations for several small molecules (see refs. [**67**] [**68**] [**21**] [**38**] and references therein), however, to our knowledge have not yet been considered so far for formaldehyde. It has been argued in many previous works [**69**] [**70**] [**71**] [**72**] [**73**] [**74**] that dynamic electron correlations beyond single and double excitations are important to approach ~~the~~ spectroscopic accuracy. They have been included in recent spectroscopically accurate PESs of methane [**12**] [**75**], whereas Morgan et al. [**13**] have reported a very thorough study of the impact of triple and quadruple excitations to the equilibrium geometry and the quartic force field of formaldehyde.

In this work, we calculated MVD corrections with MOLPRO on the full reference grid $G^{(R)}$ of 22509 points. Much more expensive calculations for DBOC and HODEC corrections were carried out at 2000 points of a smaller grid $G^{(Corr)}$ of nuclear geometries and approximated by a 4^{th} order expansion of the type (2). This gave a quite smooth analytical function of all six symmetrized coordinates for the sum of these three corrections:

$$\Delta_{(3corr)}(S_i) = \Delta_{Rel}(S_i) + \Delta_{DBOC}(S_i) + \Delta_{T(Q)}(S_i). \quad (4)$$

The DBOC and HODEC corrections were calculated using the CFOUR program suite [**76**] with the cc-pVTZ one-particle basis set. The HODEC corrections on the $G^{(Corr)}$ grid were computed using the noniterative quadruple CCSDT(Q) method [**71**] [**72**] [**73**] [**74**]. At this step we have constructed the *ab initio* corrected surface

$$PES(ACV5Z+3Corr) = PES(ACV5Z) + \Delta_{(3corr)}(S_i) \quad (5)$$

Table 5 gives the energy levels using the PES(ACV5Z) and PES(ACV5Z+3Corr) that account for the above considered corrections, analytically extrapolated from the sparser grid $G^{(Corr)}$.

It is seen that a values of the HODEC dynamic correction for formaldehyde computed with the CCSDT(Q) method is several times larger than those for the methane molecule [**12**] . The differences between the calculated and measured levels are considerably larger for the v_2 overtones. Although the PES (ACV5Z + 3Corr) for formaldehyde is constructed in a similar way as the PES for methane, its accuracy is significantly lower than that for methane. It was necessary to improve the potential energy surface, particularly along the CO bond.

Since the relativistic corrections and DBOC are relatively small, we have tried to explore further contributions related to HODEC correlations including quadruple excitations, as well as to the larger, aug-cc-pCV6Z basis set. To this end we used at the next step the iterative CCSDTQ [**73**] [**74**] [**76**] method which is expected to provide more rigorous account for dynamic electronic correlations corresponding to quadruple excitations. However, this method converged very slowly for low-symmetry geometries or for large r_{CO} bond distances. Full PES calculations at this level of the theory are extremely demanding, but it was possible to study the corresponding contributions on the most relevant one-dimensional cuts. Previous experiences in the PES corrections for various molecules showed that corrections performed along chemical bonds provide a maximum contribution. Note that for formaldehyde, all geometries keep the C_{2v} symmetry while changing the r_{CO} bond length, whereas they have the C_S symmetry while changing the r_{CH} bond length. The correction Δ_Q = CCSDTQ - CCSDT(Q) was evaluated for about twenty points along both bond stretching coordinates. The one-dimensional Δ_{AC6Z} = ACV6Z-ACV5Z corrections were also computed at the same sets of geometries. The one-dimensional corrections of the CO cut of the potential are shown in Figure 4. These corrections result in an increase of the potential energy at distances longer than r_e(CO). At the distances shorter than r_e(CO), the potential energy slightly decreases. For the r_{CO} bond, the Δ_Q = CCSDTQ-CCSDT(Q) correction in the VTZ basis considerably exceeds the Δ_{AC6Z} = ACV6Z-ACV5Z correction calculated with the CCSD(T) technique. For the r_{CH} bond, the contributions of these corrections are of a similar magnitude. We summarized two corrections $\Delta_{Q+6Z} = \Delta_Q + \Delta_{AC6Z}$ and approximated it analytically as a power series expansion in Morse-type functions Δ_{Q+6Z} (S_1,S_2,S_5) of radial coordinates (2b). The choice of analytical representations had a marginal effect on vibrational energy levels.

Our final ab intio PES including these four corrections was constructed as

$$\text{PES(ACV5Z+4Corr)} = \text{PES(ACV5Z)} + \Delta_{(3corr)}(S_i) + \Delta_{Q+6Z}(S_1,S_2,S_5) \qquad (6)$$

The fourth correction Δ_{Q+6Z} improves the accuracy of the calculated fundamental frequencies and brings them closer to the measured values, especially for v_2. Also, the correction diminished the calculated value of the equilibrium geometry r_{COe} . Contrary to the r_{CO} correction, the r_{CH} correction does have a significant effect on the energy levels. The partial contributions of the

considered corrections to vibrational energies and the values of the deviations are shown in Figure 6.

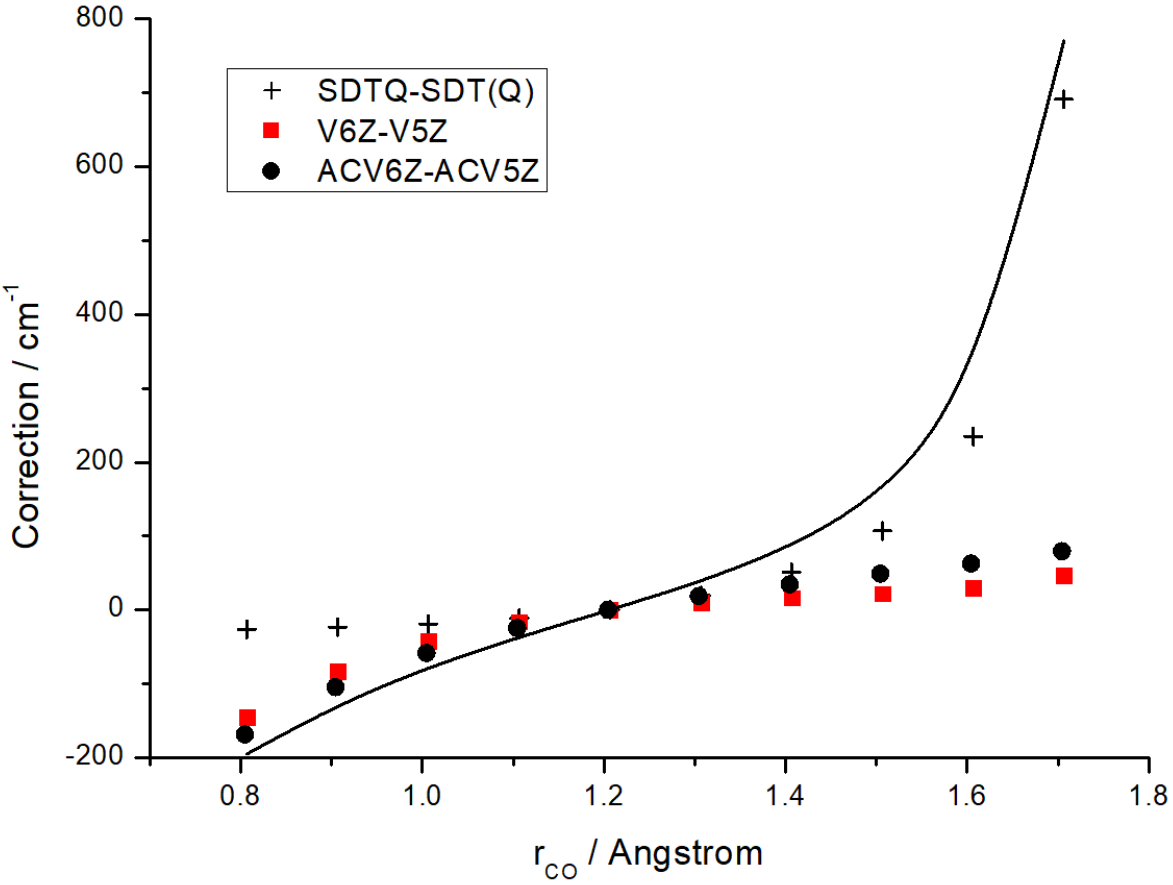

Figure 4 *One-dimensional radial corrections along the CO bond(shown as solid line). The contributions Δ_Q = CCSDTQ - CCSDT(Q) - the rigorous account for connected quadruple excitations in dynamic electron correlation - are shown as black crosses, while the Δ_{AC6Z} =(ACV6Z-ACV5Z) and Δ_{V6Z} = (V6Z-V5Z) corrections calculated at the CCSD(T) level are shown as circles and squares, respectively. The sum of two corrections $\Delta_{Q+6Z} = \Delta_Q + \Delta_{AC6Z}$ shown as a solid line.*

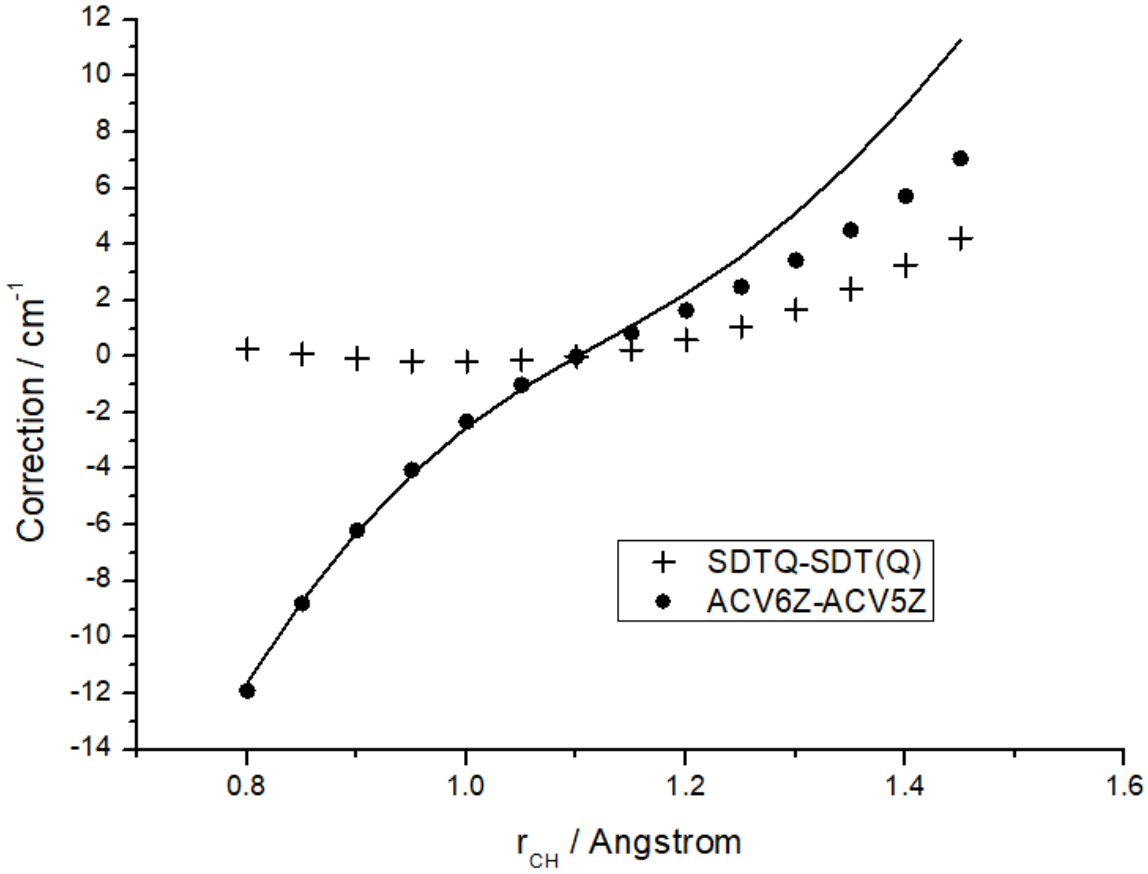

Figure 5 *One-dimensional radial corrections along the CH bond (shown as solid line). The contributions Δ_Q = CCSDTQ - CCSDT(Q) - the rigorous account for connected quadruple excitations in dynamic electron correlation - are shown as black crosses, while the Δ_{AC6Z} = (ACV6Z-ACV5Z) correction calculated at the CCSD(T) level is shown as circles. The sum of two corrections Δ_{Q+6Z} = Δ_Q + Δ_{AC6Z} shown as a solid line.*

The contributions of various corrections to vibrational levels and our final ab initio results are collected in Table 5. The experimental energy levels are taken from refs [**77**] [**78**] [**79**], and [**80**]. Note that the (Exp.-Calc.) deviations exceed 1 cm^{-1} only for six levels among a total of 35 experimentally known levels. The deviation of -1 cm^{-1} for $2\nu_2$ is quite reasonable considering that the deviation for ν_2 is equal to -0.44 cm^{-1}. Four levels from the other five have been taken from ref [**80**]. This work reported the level values with only one significant digit after the decimal point. Ref [**79**] reported another vibrational band center $\nu_2 + \nu_4 + \nu_6$ derived from 40 rotational-vibrational energy levels including J values up to 17 with an uncertainty of 0.33 cm^{-1}. Unfortunately, this work [**79**] did not mention a minimum value of J for experimental transitions in the $\nu_2 + \nu_4 + \nu_6$ band. If the fitting procedure does not use a sufficient number of the assigned transitions with J < 6, the accuracy of the extrapolated empirical J=0 level might be poor. A large difference can be explained by the fact that the two calculations deviate in different directions. Four other band centers above 4400 cm^{-1} have been reported in ref [**79**]: $\nu_1+\nu_2$ at 4529.5025(50) cm^{-1}, $\nu_2+\nu_5$ at 4571.6947(50) cm^{-1}, $2\nu_2+\nu_6$ at 4734.2078(50) cm^{-1}, and $3\nu_2$ at 5177.75952(70) cm^{-1}. The corresponding calculated levels at 4530.19, 4571.72, 4734.95, and 5179.37 cm^{-1} are slightly higher than the empirical values, but the most significant part of the

overestimation is due to the deviation of ν_2 levels, which can be roughly estimated as -0.44n where n is number of ν_2 quanta.

Table 5. Vibrational levels with contributions of relativistic, DBOC corrections, and high-order electron correlations up to 4400 cm^{-1}.

Vib. State	C	Exp. levels *	This work								ref. [**14**]	
			Contributions of corrections #				Theoretical levels with corrections				Calc	Exp-Calc
			Rel.	DBOC	T(Q)	Q+6Z	ACV5Z	ACV5Z +3corr	ACV5Z +4corr	Exp-Calc ##		
ν_4	B_1	1167.25628(2)[a]	-0.14	-0.07	-3.82	0.55	1170.469	1166.43	1166.99	0.27	1166.1	1.16
ν_6	B_2	1249.09568(2)[a]	-0.06	0.08	-2.24	0.65	1250.471	1248.25	1248.91	0.18	1245.6	3.49
ν_3	A_1	1500.17574(12)[a]	0.06	-0.13	-2.28	0.76	1501.967	1499.62	1500.38	-0.21	1499.1	1.07
ν_2	A_1	1746.00886(13)[a]	-0.91	-0.23	-8.86	3.75	1752.703	1742.69	1746.45	-0.44	1744.61	1.4
$2\nu_4$	A_1	2327.5239(5)[b]	-0.28	-0.14	-7.59	1.10	2333.903	2325.89	2326.99	0.53	2325.18	2.35
$\nu_4 + \nu_6$	A_2	2422.9701(50)[b]	-0.21	0.00	-6.10	1.22	2427.594	2421.29	2422.52	0.45	2418.43	4.54
$2\nu_6$	A_1	2494.3543(5)[b]	-0.13	0.15	-4.49	1.32	2497.191	2492.71	2494.03	0.32	2487.73	6.63
$\nu_3 + \nu_4$	B_1	2667.0481(20)[b]	-0.09	-0.19	-6.18	1.33	2672.132	2665.67	2667.00	0.05	2664.64	2.4
$\nu_3 + \nu_6$	B_2	2719.1550(5)[b]	-0.03	-0.15	-4.43	1.04	2722.697	2718.08	2719.13	0.03	2715.24	3.92
ν_1	A_1	2782.4575(5)[b]	-0.25	-0.61	-4.78	0.34	2788.101	2782.46	2782.81	-0.35	2781.74	0.71
ν_5	B_2	2843.3256(5)[b]	-0.37	-0.37	-6.14	0.90	2848.961	2842.08	2842.98	0.34	2842.37	0.95
$\nu_2 + \nu_4$	B_1	2905.9685(20)[b]	-1.06	-0.30	-12.8	4.34	2916.043	2901.80	2906.14	-0.18	2903.35	2.61
$2\nu_3$	A_1	2998.9873(5)[b]	0.11	-0.25	-4.69	1.55	3002.723	2997.89	2999.44	-0.46	2997.24	1.74
$\nu_2 + \nu_6$	B_2	3000.0659(5)[b]	-0.88	-0.19	-10.4	3.98	3007.897	2996.34	3000.32	-0.26	2995.91	4.16
$\nu_2 + \nu_3$	A_1	3238.4548(20)[b]	-0.89	-0.36	-11.3	4.62	3247.114	3234.49	3239.10	-0.65	3236.11	2.35
$2\nu_2$	A_1	3471.6	-1.81	-0.46	-17.8	7.58	3485.266	3465.10	3472.69	-1.09	3469.39	2.21
$3\nu_4$	B_1	3480.7	-0.41	-0.21	-11.3	1.65	3491.059	3479.11	3480.76	-0.06	3478.04	2.66
$2\nu_4 + \nu_6$	B_2	3586.6	-0.35	-0.06	-9.82	1.77	3594.654	3584.42	3586.19	0.41	3581.09	5.51
$\nu_4 + 2\nu_6$	B_1	**3673.5**[$]	-0.28	0.07	-8.42	1.86	3682.802	3674.16	3676.03	-2.53	3668.88	4.62
$3\nu_6$	B_2	-	-0.21	0.20	-6.79	1.89	3740.452	3733.65	3735.54	-	-	-
$\nu_3 + 2\nu_4$	A_1	3825.3	-0.24	-0.26	-9.98	1.89	3834.334	3823.86	3825.74	-0.45	3822.43	2.87
$\nu_3 + \nu_4 + \nu_6$	A_2	**3886.5**[$]	-0.21	-0.25	-8.39	1.50	3895.439	3886.59	3888.10	-1.60	3883.37	3.13
$\nu_3 + 2\nu_6$	A_1	**3937.4**[$]	-0.14	-0.14	-6.77	1.49	3940.654	3933.60	3935.09	2.31	3929.86	7.54
$\nu_1 + \nu_4$	B_1	3941.5295[c]	-0.40	-0.66	-8.83	0.89	3950.568	3940.68	3941.57	-0.04	3939.85	1.68
$\nu_4 + \nu_5$	A_2	3996.518[c]	-0.49	-0.40	-9.94	1.48	4005.302	3994.47	3995.94	0.57	3994.75	1.77
$\nu_1 + \nu_6$	B_2	4021.0806(6)[d]	-0.31	-0.50	-7.17	1.00	4028.157	4020.18	4021.18	-0.10	4017.7	3.38
$\nu_2 + 2\nu_4$	A_1	4058.3	-1.18	-0.36	-16.5	4.84	4071.474	4053.43	4058.28	0.02	4054.6	3.7
$\nu_5 + \nu_6$	A_1	4083.1	-0.52	-0.21	-9.30	2.07	4090.512	4080.47	4082.54	0.56	4078.88	4.22
$\nu_2 + \nu_4 + \nu_6$	A_2	**4163.289(330)**[d,$]	-1.06	-0.26	-14.6	4.66	4176.049	4160.08	4164.74	-1.45	4159.35	3.94
$2\nu_3 + \nu_4$	B_1	-	-0.05	-0.31	-8.65	2.13	4172.264	4163.25	4165.37	-	-	-
$2\nu_3 + \nu_6$	B_2	4192.3816(5)[d]	0.00	-0.33	-6.74	1.54	4198.047	4190.96	4192.51	-0.13	4189.62	2.77
$\nu_2 + 2\nu_6$	A_1	4248.7	-0.87	-0.15	-12.2	4.27	4256.837	4243.52	4247.79	0.90	4241.02	7.68
$\nu_1 + \nu_3$	A_1	**4253.8**[$]	-0.18	-0.72	-7.00	1.07	4262.684	4254.79	4255.86	-2.06	4253.86	-0.06

$\nu_3 + \nu_5$	B_2	4335.0971(6)[d]	-0.30	-0.42	-8.69	1.90	4342.566	4333.15	4335.05	0.05	4334.78	0.32
$\nu_2 + \nu_3 + \nu_4$	B_1	4397.5	-1.05	-0.43	-15.4	5.22	4409.877	4392.92	4398.14	-0.64	4394.05	3.45
RMS deviation										0.40		1.54
RMS (-5 lev.) [$]										0.21		1.67

*) Experimental values given in wavenumber units (cm^{-1}), a – from ref [**81**], b – from ref [**78**], c – from ref [**77**], d – from ref [**79**], with one decimal place from ref [**80**].

#) Rel.= relativistic; T(Q) = CCSDT(Q) – CCSD(T) correlation; Q+6Z = quadruple Δ_{Q+6Z} correction (see text for explanation).

##) Experimental minus calculated levels corresponding to the full ab initio PES(ACVZ6 + 4Corr).

[$]) RMS without five suspicious levels given in Table 6.

Note that most of the "outlier" levels in our (exp.-calc.) with deviations larger than 1 cm^{-1} also showed significant deviations from empirical values in calculations of Burleigh et al. [**15**] and of Yachmenev et al. [**14**]. Table 6 compares three calculations for these five levels.

Table 6. Five vibrational levels from Table 5 with our (Exp.-Calc.) deviations exceeding 1 cm^{-1}.

Vib. State	C	**Exp. ***	This work		ref. [**15**]		ref. [**14**]	
$\nu_4 + 2\nu_6$	B_1	**3673.5**[?]	3676.032	-2.53	3675.9	-2.4	3675.07	−1.57
$\nu_3 + \nu_4 + \nu_6$	A_2	**3886.5**[?]	3888.101	-1.60	3886.7	-0.2	3886.47	0.03
$\nu_3 + 2\nu_6$	A_1	**3937.4**[?]	3935.095	2.31	3935.4	2.0	3936.02	1.38
$\nu_2 + \nu_4 + \nu_6$	A_2	**4163.289**[?]	4164.739	-1.45	4163.6	0.3	4164.12	−0.83
$\nu_1 + \nu_3$	A_1	**4253.8**[?]	4255.859	-2.06	4255.3	-1.5	4254.58	−0.78

*) experimental values reported in refs [**80**], [**79**]

Note that empirical levels reported by Bouwens et al. [**80**] in 1996 have been obtained from low resolution dispersed fluorescence spectra with an average uncertainty of 1 cm^{-1}. However, some of these empirical levels could have larger errors as they differ considerably from values obtained from high-resolution spectra analyses in more recent papers. For example, the study of Bouwens et al [**80**] reported the $\nu_3 + \nu_6$ level at 2496.11 cm^{-1} and the $\nu_1 + \nu_4$ level at 3940.21 cm^{-1}. In a more recent paper of A. Perin et al. [**78**] [**81**] the same levels were obtained from analyses of vibration-rotation spectra at 2494.3543 cm^{-1} and at 3941.5295 cm^{-1}, respectively. Figure 7 shows the diagram illustrating the differences between empirical levels obtained from dispersed fluorescence spectra [**80**] and those obtained from infrared rotationally resolved spectra [**78**] [**81**]. A comparison of fundamental band centers computed from our final ab initio PES including all corrections with the results of the recent, very thorough study by Morgan et al [**13**] is given in Table 7. According to notations of ref [**13**], here MAE ($\frac{1}{n}\sum_{i=1}^{n}|X_i - Y_i|$) is the mean

411 (Exp.-Calc.) deviation, while MAPE ($\frac{100\%}{n}\sum_{i=1}^{n}\left|\frac{X_i - Y_i}{X_i}\right|$) is the mean absolute percent error

412 defined by Eq.(17) of ref [**13**].

413

414

415 **Table 7. Experimental minus calculated deviations for fundamentals of H_2CO.**

Vib. State	C	Exp.	Exp-Calc This Work	Morgan [**13**] CCSDT(Q) /CBS	Morgan [**13**] CCSDT(Q) /CBS+Rel
ν_4	B_1	1167.256	0.27	-0.8	-0.95
ν_6	B_2	1249.095	0.18	0.03	-0.08
ν_3	A_1	1500.175	-0.21	-0.03	0.01
ν_2	A_1	1746.009	-0.44	-0.32	-1.48
ν_1	A_1	2782.457	-0.35	1.18	0.49
ν_5	B_2	2843.326	0.34	1.06	0.25
MAE			0.29	0.57	0.54
MAPE(%)			0.016	0.029	0.034
RMS			0.31	0.73	0.75

416 All values are given in cm^{-1}.

417

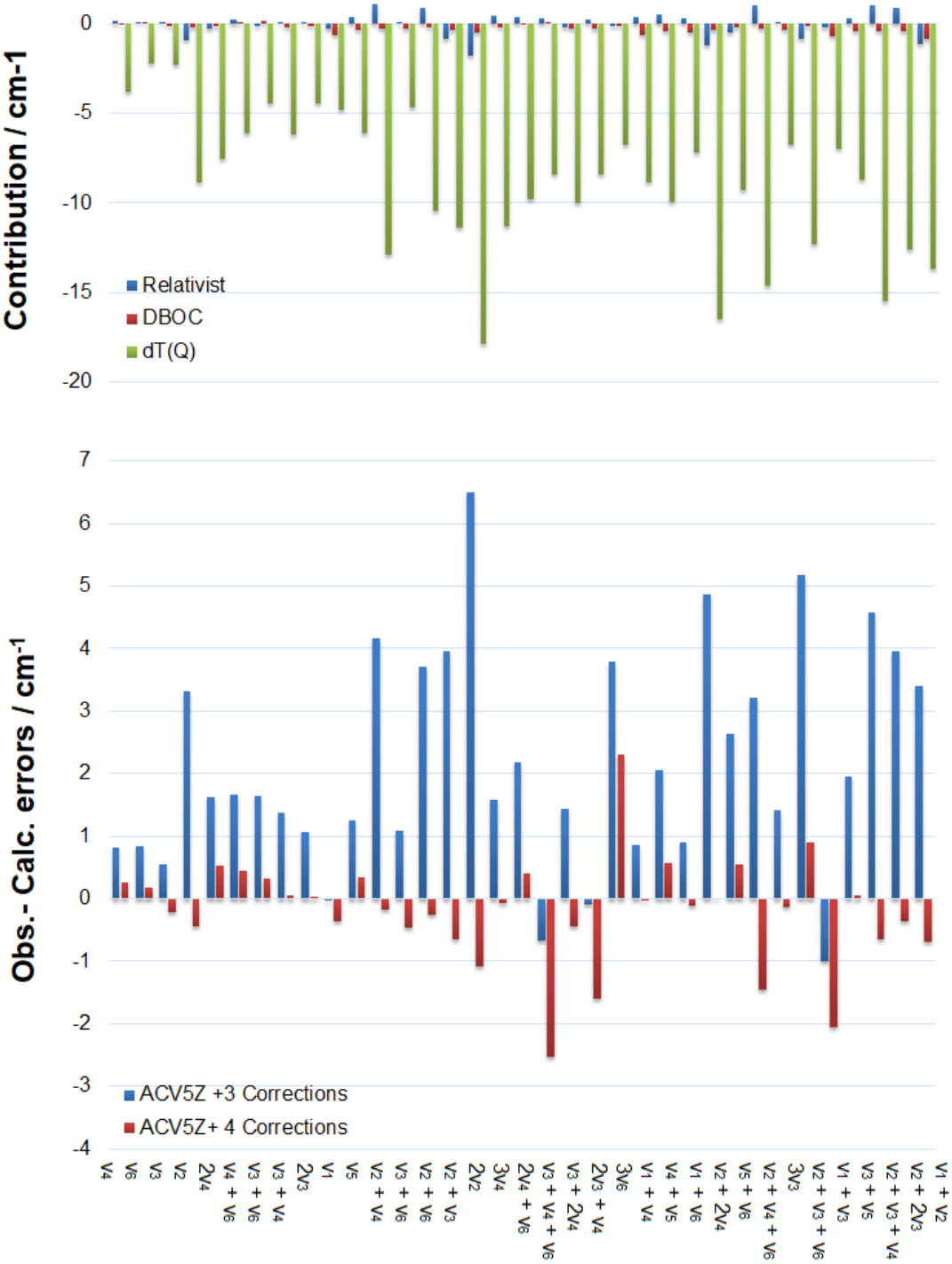

Fig 6. Upper panel(a): contribution of relativistic effects, DBOC, and high-order electron correlations T(Q) to vibrational energies up to 4500 cm^{-1}. Lower panel(b): Experimental – calculated deviations for vibration levels corresponding to ab initio calculations using PES (ACV5Z+3Corrections) in blue and to PES(ACV5Z+4Corrections) in red. Both vertical scales are given in cm^{-1}.

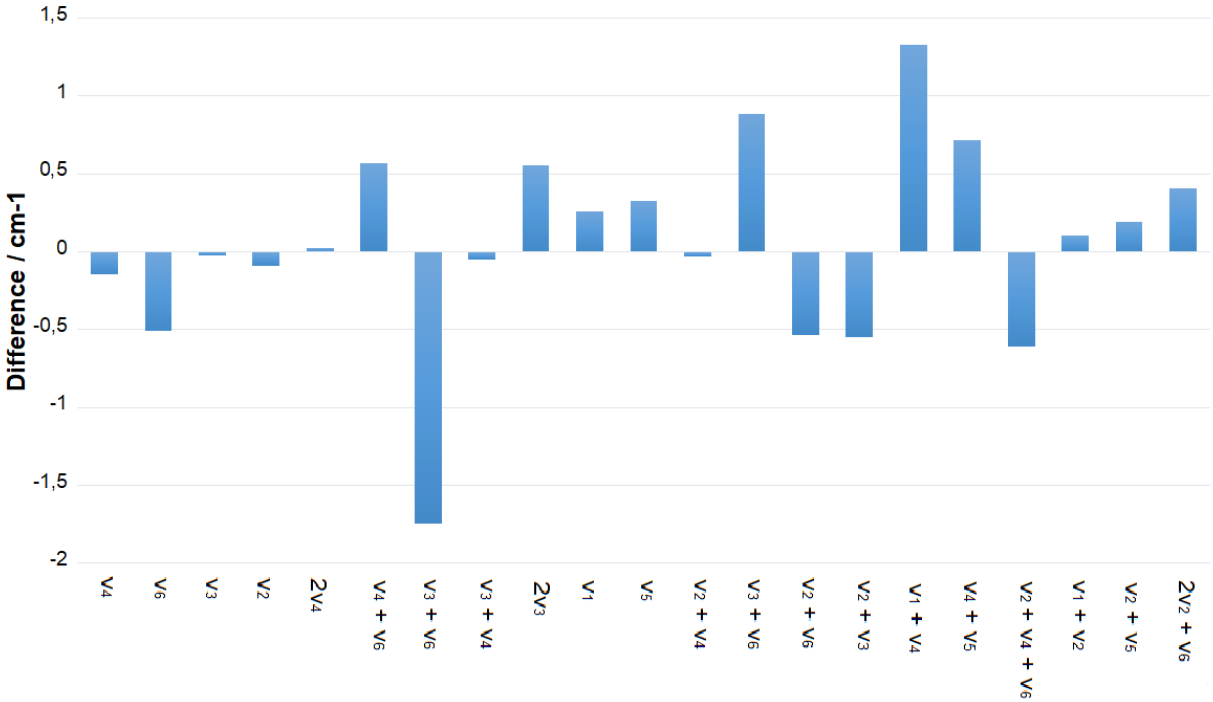

Fig 7. Exp.(HighRes)-Exp.(LowRes) , where Exp(HighRes) refers to vibrational levels obtained from high resolution spectra analyses in the infrared range [**78**] [**82**] [**79**]*, whereas Exp.(LowRes) corresponds to low resolution dispersed fluorescence data reported by Bouwens et al* [**80**] *. Vertical scales are given in* cm^{-1}.

In order to improve the accuracy of vibrational predictions, we have also produced an empirically optimized PES, by a fitting of 6 harmonic ~~second order~~ terms of the potential expansion to 20 levels experimentally determined with three decimal digits (reported in Table 5 excepting the level at 4163.289 cm^{-1}). With this fine tuning of the six PES parameters, the RMS (exp.-calc.) deviation for 20 accurate levels derived from high-resolution spectra fall down from 0.21 cm^{-1} to 0.008 cm^{-1}. Figure 8 shows the diagram of differences between the experimental levels and those calculated from our best ab initio PES and from the empirically optimized PES.

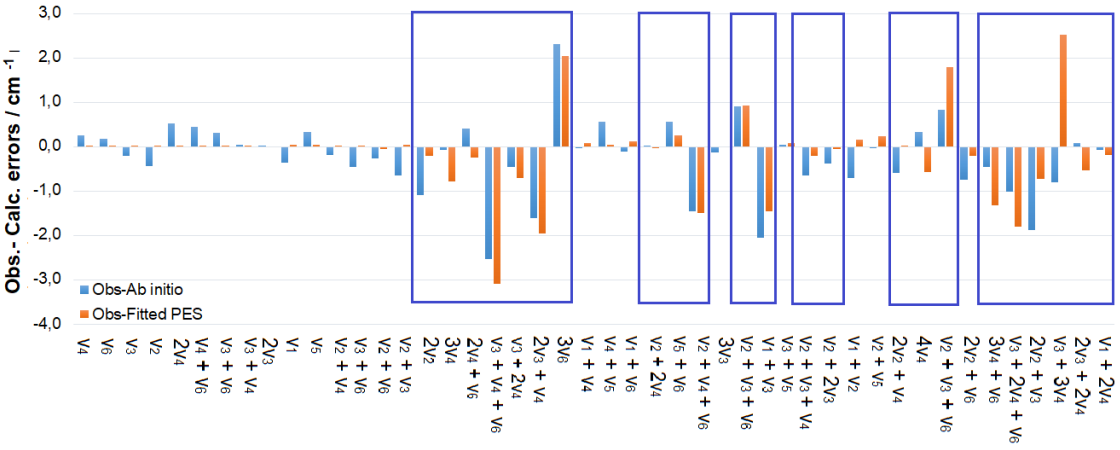

Fig 8. Experimental minus calculated deviations for vibrational levels computed from pure ab initio PES(ACV5Z+4Corr) and from the empirically optimized PES. Vertical scales are given in cm^{-1}. *Levels from Bouwens et al.* [**80**] *and the suspicious level* $v_2 + v_4 + v_6$ *from* [**79**] *are*

displayed in rectangles. Only known vibrational levels up to 5100 cm^{-1} are represented on the horizontal axis.

The experimental values derived from low resolution dispersed fluorescence spectra of Bouwens et al [**80**], for which the accuracy is considerably lower than for levels obtained from analyses of rotationally resolved infrared spectra using an effective Hamiltonian technique, are shown in the rectangular frame. It is seen that without the levels in the frames, the errors of our ab initio levels are smaller than the discrepancies between the low resolution data of Bouwens et al [**80**] and the experimental levels obtained in more recent works (see Figure 7). It can thus be concluded that the accuracy of our final ab initio calculations is not worse than that of low resolution experimental levels reported in [**80**], at least for the bands with doubly and triply excited vibrational quanta. Energy levels up to 7000 cm-1, calculated from our empirically fitted PES in orthogonal coordinates are shown in the first column of Table 8. These coordinates permit using the KEO, which is considered as "exact" (not requiring series expansion), however the latter term is only meaningful within the framework of the Born-Oppenheimer approximation. In order to calculate energy levels in normal coordinates the energy values generated from the analytical form of the PES in orthogonal coordinates were computed on our $G^{(R)}$ grid of geometries (see paragraph 2) and then re-fitted in internal coordinates with the torsion function of (τ - π). The TENSOR code [**83**] [**84**] [**85**] [**86**] was then used to calculate the energy levels in normal coordinates using the Watson-Eckart KEO. Most likely, the accuracy of the levels computed from empirically optimized PES for doubly and triply excited quanta is higher than the accuracy of the levels obtained using the pure ab initio PES. However, in case of the bands corresponding to four or more vibrational quanta, the error caused by an empirical correction might be larger than that for levels obtained using the initial ab initio PES, because only 20 low energy experimental levels were included in the fit. Note that four band centers $\nu_1+ \nu_2$, $\nu_2+ \nu_5$, $2\nu_2+\nu_6$, and $3\nu_2$ were not used in fit of the PES, but the corresponding energy levels calculated from empirically optimized PES became noticeably (RMS four times lower) closer to the empirical values. The difference between the two calculations in Table 8 is several times bigger than the initial difference between the corresponding Calc 3 and Calc 4 results for the ab initio V5Z PES (figure 3), although the calculations are converged in both cases. This could occur due to the limited order of the PES expansion and to numerical issues in the procedure of the coordinate transformations on a final grid of points. For this reason, the predicted values of high-energy levels in Table 8 have to be taken with caution. They could be useful in the initial steps of the assignment, if no other, more precise values are available.

Table 8 . Vibrational levels (in cm^{-1}) of the main formaldehyde isotopologue H_2CO computed from our empirically optimized PES using two sets of coordinates with two versions of variational calculations.

Sym, vib labels*	Calc A [#]	Calc B [##]	Difference (A-B)
B1 000100	1167.263	1167.247	0.016
B2 000001	1249.103	1249.044	0.059
A1 001000	1500.140	1500.138	0.002
A1 010000	1746.002	1746.005	-0.003
A1 000200	2327.519	2327.492	0.027
A2 000101	2422.989	2422.912	0.076
A1 000002	2494.406	2494.293	0.113
B1 001100	2667.030	2667.017	0.014
B2 001001	2719.222	2719.197	0.026
A1 100000	2782.492	2782.499	-0.008
B2 000010	2843.343	2843.311	0.032
B1 010100	2905.969	2905.958	0.011
A1 002000	2998.953	2998.941	0.012
B2 010001	3000.159	3000.110	0.049
A1 011000	3238.402	3238.407	-0.005
A1 020000	3471.801	3471.806	-0.005
B1 000300	3481.518	3481.485	0.033
B2 000201	3586.906	3586.813	0.093
B1 000102	3676.685	3676.568	0.117
B2 000003	3736.082	3735.927	0.155
A1 001200	3826.023	3825.994	0.030
A2 001101	3888.514	3888.480	0.034
A1 001002	3935.451	3935.337	0.114
B1 100100	3941.539	3941.542	-0.004
A2 000110	3996.548	3996.503	0.045
B2 100001	4021.081	4021.039	0.041
A1 010200	4058.360	4058.336	0.024
A1 000011	4082.935	4082.874	0.061
A2 010101	4164.835	4164.773	0.062
B1 002100	4165.153	4165.135	0.018
B2 002001	4192.437	4192.407	0.030
A1 010002	4247.860	4247.772	0.087
A1 101000	4255.327	4255.329	-0.002
B2 001010	4335.077	4335.028	0.049
B1 011100	4397.710	4397.703	0.007
B2 011001	4466.891	4466.869	0.022
A1 003000	4495.549	4495.533	0.016
A1 110000	4529.420	4529.457	-0.037
B2 010010	4571.525	4571.519	0.006
B1 020100	4624.282	4624.281	0.001
A1 000400	4629.634	4629.602	0.032
A1 012000	4729.001	4728.995	0.006
B2 020001	4734.453	4734.419	0.035
A2 000301	4743.299	4743.198	0.101
A1 000202	4843.901	4843.775	0.126
A2 000103	4928.842	4928.695	0.147
A1 021000	4955.909	4955.924	-0.015

A1 000004	4974.735	4974.536	0.199
B1 001300	4978.413	4978.371	0.042
B2 001201	5044.315	5044.276	0.039
A1 100200	5092.702	5092.730	-0.027
B1 001102	5111.129	5111.015	0.114
B2 000210	5140.810	5140.722	0.088
B2 000012	5151.476	5151.302	0.175
A1 030000	5178.050	5178.078	-0.028
A2 100101	5186.406	5186.361	0.045
B1 010300	5205.475	5205.445	0.029
B1 001102	5246.933	5246.868	0.066
A1 100002	5253.556	5253.499	0.058
B2 010201	5312.412	5312.323	0.089
A1 002200	5322.146	5322.106	0.041
B2 010201	5325.537	5325.463	0.074
A2 002101	5359.048	5359.007	0.041
A1 001011	5383.971	5383.855	0.116
B1 101100	5414.636	5414.625	0.011
B1 010102	5419.717	5419.635	0.082
B2 100010	5433.111	5433.318	-0.207
A1 200000	5463.113	5463.393	-0.281
A2 001110	5490.220	5490.169	0.051
B2 010003	5490.308	5490.176	0.131
B2 101001	5530.358	5530.434	-0.075
A1 011200	5544.288	5544.261	0.026
A1 011200	5552.705	5552.692	0.013
A2 011101	5627.353	5627.327	0.026
A1 000020	5651.311	5651.317	-0.007
B1 003100	5660.831	5660.816	0.015
B2 003001	5665.587	5665.536	0.051
B1 110100	5681.295	5681.319	-0.025
A1 011002	5687.375	5687.256	0.119
A2 010110	5718.950	5718.932	0.018
A1 102000	5729.450	5729.448	0.002
B2 110001	5765.234	5765.242	-0.008
A1 020200	5769.551	5769.541	0.010
B1 000500	5772.142	5772.133	0.009
A1 010011	5809.358	5809.322	0.036
B2 003001	5822.554	5822.520	0.033
B1 012100	5887.355	5887.344	0.011
A2 020101	5889.405	5889.373	0.032
B2 000401	5892.767	5892.686	0.081
B2 012001	5935.857	5935.799	0.057
A1 020002	5985.373	5985.326	0.046
A1 004000	5988.654	5988.651	0.003
A1 111000	5997.360	5997.369	-0.009
B1 000302	6002.841	6002.727	0.113
B2 011010	6052.566	6052.564	0.002
B2 000203	6097.490	6097.335	0.155
B1 021100	6107.429	6107.441	-0.012
A1 001400	6124.578	6124.543	0.034
B1 000104	6180.301	6180.124	0.177
A2 000310	6190.937	6190.917	0.020

B2 021001	6196.629	6196.618	0.011
B2 000005	6211.767	6211.549	0.218
A1 013000	6216.906	6216.889	0.017
B1 100300	6236.880	6236.997	-0.117
A1 120000	6254.983	6255.058	-0.075
A1 000211	6265.909	6265.782	0.127
B2 020010	6275.837	6275.861	-0.024
A2 000310	6283.377	6283.364	0.013
B1 030100	6322.849	6322.896	-0.047
A2 000112	6335.338	6335.170	0.168
B2 100201	6340.507	6340.531	-0.024
A1 010400	6346.545	6346.522	0.022
A1 000013	6360.567	6360.303	0.264
A1 001202	6401.440	6401.405	0.036
B1 100102	6426.649	6426.645	0.004
A1 022000	6437.667	6437.681	-0.014
B2 030001	6451.851	6451.859	-0.008
A2 010301	6466.652	6466.599	0.053
B1 002300	6472.643	6472.596	0.047
B2 100003	6476.996	6476.944	0.052
A2 001103	6495.501	6495.445	0.056
B2 001210	6510.481	6510.441	0.039
A1 001004	6546.991	6546.894	0.097
B1 001111	6553.062	6553.068	-0.006
A1 101200	6564.842	6564.913	-0.071
B2 001012	6578.550	6578.313	0.237
A1 010202	6580.280	6580.214	0.066
A2 100110	6584.443	6584.991	-0.548
B1 200100	6612.308	6612.932	-0.624
A1 100011	6629.339	6629.655	-0.317
B2 002201	6636.922	6636.909	0.013
A1 031000	6653.251	6653.314	-0.062
A2 010103	6670.621	6670.512	0.109
A2 101101	6683.934	6684.163	-0.229
B2 200001	6684.586	6685.095	-0.509
B1 011300	6693.205	6693.178	0.027
B1 002102	6708.592	6708.624	-0.032
A1 010004	6727.367	6727.179	0.188
B2 002003	6758.622	6758.625	-0.003
A1 101002	6766.827	6767.112	-0.285
B2 011201	6778.065	6778.064	0.001
B1 000120	6795.388	6795.461	-0.074
A1 003200	6813.391	6813.333	0.057
A1 110200	6825.366	6825.462	-0.096
A2 002110	6829.984	6829.955	0.030
A1 002011	6838.098	6838.072	0.026
B1 011102	6851.401	6851.322	0.079
B2 010210	6856.265	6856.337	-0.071
B2 101010	6864.634	6865.029	-0.395
A1 040000	6865.517	6865.643	-0.126
B1 102100	6888.866	6888.915	-0.049
B2 011003	6894.266	6894.350	-0.083
B2 010012	6904.180	6903.974	0.206

A1 000600	6909.239	6909.337	-0.098
B1 020300	6909.809	6909.812	-0.003
A1 201000	6914.801	6915.485	-0.684
A2 110101	6922.631	6922.694	-0.063
B1 011102	6966.384	6966.388	-0.003
A2 003101	6978.675	6978.675	0.000
A1 110002	6990.034	6990.107	-0.074

**) Vibrational state labels include C_{2v} symmetry types and normal mode vibrational assignment.*
#) Calc A. corresponds to direct calculations using our empirically optimized PES in orthogonal coordinates (I) and the torsion functions cos(τ/2) with the exact kinetic energy operator in polyspherical coordinates.
##) Calc B. corresponds to calculations using our empirically optimized PES refitted in normal coordinates on a geometrical grid with the Watson-Eckart kinetic energy operator.

4. Deuterated D_2CO isotopologue

The vibrational levels of D_2CO given in Table 9 were calculated, using nuclear masses, from two potential surfaces. The calculation (CalcD_2CO 1) corresponds to our best ab initio PES(ACV5Z+4Corr) and (CalcD_2CO 2) corresponds to the empirically optimized PES fitted to twenty vibrational levels of the main formaldehyde isotopologue as described in the previous section. Experimental levels were taken from refs [**82**] (the first 3 levels), [**87**] (ν2), and [**88**] (the remaining 8 levels). Note that ref [**88**] reports both the vibrational levels obtained from experimental transitions from the ground state to the upper level J=0 (see Table 3 in ref [**88**]), as well as the spectroscopic parameter of the band center derived with the least squares technique. The spectroscopic parameter of the band center and vibrational level in the same units (cm-1) should have closely lying values in the absence of anharmonic Fermi-type resonances, but could considerably differ however, in the case of a strong Fermi coupling. Table 10 of ref [**13**] erroneously gives the spectroscopic parameter 2054.694 cm^{-1} instead of the experimental vibrational level 2060.91963 cm^{-1} for ν_1. The experimental vibrational level ν_1 is considerably closer to the calculated value of ref [**13**]. In Table 9, we compare the experimental and calculated levels. Note that all calculated levels, except for $2\nu_4$, are close to experimental ones. The choice of various representations of potentials, coordinates, and the size of the vibrational basis do not have any considerable effect on the calculated energy levels given in Table 9. The D_2CO isotopologue is heavier than H_2CO, and the DBOC correction for D_2CO is expected to be less important than this correction for H_2CO. In case of D2CO (CalcD_2CO 1), the DBOC was not recalculated. To estimate the contribution of DBOC, we presented it in the form of an expansion in a second-order Taylor series. Comparison of parameters of the DBOC of the two isotopologues D2CO/H2CO shows that the contribution of DBOC_D2CO is ~ 0.6 *DBOC_H2CO. Since the contribution is weak, the -0.4 contribution for the main isotopologue (see column DBOC of Table 5) could be added to the calculated D2CO levels (CalcD_2CO 1). In

514 this case, levels ν_1 (2060.887cm^{-1}), ν_2 (1701.258 cm^{-1}), ν_5 (2162.657 cm^{-1}) would become a little
515 closer to the empirical values.

516 Since a considerable number of transitions in the $2\nu_4$ band have been assigned and accurate
517 combination differences have been derived in ref [**88**], an outlier in the $2\nu_4$ band center printed in
518 Table 3 of ref [**88**] could likely be interpreted as a misprint. On the other hand, the authors of ref
519 [**88**] have stated (the second sentence of the fourth paragraph): "One can clearly see the three
520 strong fundamental bands ν_2, ν_1, and ν_5 with the centers located near 1701.6 cm^{-1}, 2060.9 cm^{-1},
521 and 2162.9 cm-1, respectively. The weak bands $2\nu_4$, 1867.8 cm^{-1}, $\nu_4+\nu_6$, 1930.0 cm^{-1}, and $2\nu_6$,
522 1974.3 cm^{-1}, can also be recognized very clearly in spite of their weakness". These band centers
523 are close (within 0.1 cm^{-1}) to reported experimental vibrational levels of ref [**88**], except for the
524 experimental vibrational level $2\nu_4$, which was shifted by 2 cm^{-1} with respect to the band center
525 cited above. Note, that the center of the $2\nu_4$ band reported in ref [**88**] (1867.8 cm^{-1}) is very close
526 to our calculated vibrational level of $2\nu_4$ (1867.6 cm^{-1}). Figure 7 of ref [**88**] indicates the
527 presence of a Fermi resonance between the $2\nu_4$ and ν_1 bands. However, Table 6 of the same
528 paper [**88**] missed the parameter of this resonance.

529 The last row of Table 9 gives the RMS values of differences between experimental and
530 calculated levels. The empirically optimized PES provides the best description of the energy
531 levels, except for the doubted $2\nu_4$ value.

532 **Table 9. Vibrational levels for the D_2CO isotopologue up to 3000 cm^{-1}.**

Vib. State	C	Exp. levels *)	CalcD_2CO 1 ***	Exp.-CalcD_2CO 1	CalcD_2CO 2***	Exp.-CalcD_2CO 2
ν_4	B_1	938.03549	937.936	0.099	937.711	0.324
ν_6	B_2	989.25028	989.174	0.076	989.053	0.197
ν_3	A_1	1100.44254	1100.403	0.039	1100.536	-0.093
ν_2	A_1	1701.619103	1701.166	0.453	1701.631	-0.012
$2\nu_4$	A_1	1865.84444	1867.602	-1.757	1867.21	-1.365
$\nu_4+\nu_6$	A_2	1930.02676	1929.852	0.174	1929.524	0.502
$2\nu_6$	A_1	1974.32541	1974.232	0.092	1973.993	0.332
$\nu_3+\nu_4$	B_1	2038.90981	2038.801	0.108	2038.708	0.202
ν_1	A_1	2060.91963	2060.643	0.275	2060.852	0.067
$\nu_3+\nu_6$	B_2	2072.66611	2072.585	0.080	2072.509	0.157
ν_5	B_2	2162.92330	2162.509	0.414	2162.118	0.805
$2\nu_3$	A_1	2201.73284	2201.727	0.005	2201.98	-0.247
$\nu_2+\nu_4$	B_1		2633.045		2633.258	
$\nu_2+\nu_6$	B_2		2685.004		2685.288	
$\nu_2+\nu_3$	A_1		2790.027		2789.501	
RMS deviation RMS (- level $2\nu_4$) **				0.55 0.21		0.51 0.34

533 *) Experimental levels from refs [**82**] [**87**] [**88**] in cm^{-1}.

534 **) RMS deviation without the suspicious level $2\nu_4$.

535 ***) See text in the beginning of the paragraph

536

5. Conclusion

The recent thorough study of the quartic force field of the formaldehyde molecule by Morgan et al [**13**] obtained at 183 nuclear geometries near the equilibrium configuration has shown the importance of high-order dynamic electron correlation by including triple and quadruple excitations in the coupled-cluster hierarchy via the CCSDT(Q) method. This has permitted improving fundamental band origins with respect to the standard CCSD(T) approach with an RMS deviation of 0.52 cm^{-1} [**13**]. In this work, we confirm these conclusions using the algorithm of the construction of the full six-dimensional PES at an extended set of geometries. To this end, we used successive grids adapted to the level of the theory that was previously applied for the methane molecule [**12**]. These methods, including also relativistic and adiabatic DBOC corrections, allowed us to approach ~~the~~ spectroscopic accuracy in ab initio calculations for a larger range of vibrational energies. For the first time – in case of a four-atom molecule with 16 electrons like H2CO - it was possible to obtain the (ab initio – experimental) RMS deviation of 0.4 cm^{-1} including 33 experimental vibrational band origins up to three vibrational quanta (Table 6).

First-principle calculations provide an independent insight into uncertainties of available experimental data, particularly for those which had been deduced from low-resolution dispersed fluorescence spectra [**80**]. A detailed comparison of various sources in Table 7 and Figures 6-8 suggests that many experimental levels could be less accurate than the present ab initio calculations. By excluding five suspicious band origins corresponding to large experimental uncertainties, the RMS deviation of our ab initio PES for vibrational levels up to 3700 cm-1 (Table 6) drops down to 0.2 cm^{-1}. A similar accuracy is obtained for vibrational levels of the deuterated isotopologue D2CO (Table 9), confirming the reliability of the ab initio PES.

We have also produced an empirically optimized PES by adjusting six second order parameters to twenty experimental vibrational levels derived from high-resolution spectra with the (obs-calc) RMS deviation of 0.008 cm^{-1}. Computed from this PES 160 band origins of H2CO up to 7000 cm^{-1} are given in Table 8. Both the ab initio and the empirically optimized PES are provided in the Supplementary Materials as a C++ code.

For a further investigation of the corresponding accuracy issues, the ab initio PES can be used to derive effective spectroscopic models by the contact transformation method as it was done in the case of methane [**89**] [**90**] [**91**]. This will permit to accurately compute physically meaningful values of the resonance coupling parameters from ab initio surface for advanced analyses of high-resolution spectra.

SUPPLEMENTARY MATERIAL

See supplementary material for the ab initio and the empirically optimized PES in orthogonal coordinates.

ACKNOWLEDGMENTS

The support of RFBR grant (Grant No. 19-03-00581) is acknowledged. V.T. acknowledges the support from Academic D.Mendeleev program of Tomsk State University and M.R. form LEFE CHAT CNRS program.

References

[1] Barbe A., Marche´ P., Secroun C., Jouve P., Measurements of tropospheric and stratospheric H2CO by an infrared high resolution technique. *J. Geophys. Res. Lett.* 1979;6: 463–465.

[2] Khare P., Kumar N., Kumari K.M., Srivastave S.S., Atmospheric formic and acetic acids: An overview. *Rev. Geophys.* 1999;37: 227.

[3] Kakabokas P., Carlier P., Fresnet P., Mouvierg G., Toupance G., Field studies of aldehyde chemistry in the Paris area. *Atmos. Environ.* 1988;22: 147-155.

[4] Zhu L., Abad G.G., Nowlan C.R., Miller C.C., Chance K, Ape E.C., DiGangi J.P., Fried A., Hanisco T.F., Hornbrook R.S., Hu L., Validation of satellite formaldehyde (HCHO) retrievals using observations from 12 aircraft campaigns *Atmos. Chem. Phys.* 2020;20: 12329–12345.

[5] Steck T., Glatthor N., Von Clarmann T., Fischer H., Flaud J.M., Funke B., Grabowski U., Höpfner M., Retrieval of global upper tropospheric and stratospheric formaldehyde (H2CO) distributions from high-resolution MIPAS-Envisat spectra *Atmospheric Chemistry and Physics* 2008;8: 463-470.

[6] Dufour G., Szopa S., Barkley M.P., Boone C.D., Perrin A., Palmer P.I., Bernath P.F., Global upper-tropospheric formaldehyde: Seasonal cycles observed by the ACE-FTS satellite instrument *Atmospheric Chemistry and Physics* 2009;9: 3893-3910.

[7] Rey M., Nikitin A.V., Tyuterev V.G., Accurate Theoretical Methane Line Lists in the Infrared up to 3000 K and Quasi-continuum Absorption/Emission Modeling for Astrophysical Applications *Astrophysical journal* 2017;847: 105.

[8] Rey M., Nikitin A.V., Campargue A., Kassi S., Mondelain D., Tyuterev Vl.G., Ab initio variational predictions for understanding highly congested spectra: Rovibrational assignment of 108 new methane sub-bands in the icosad range (6280-7800 cm-1) *Phys. Chem.Chem. Phys.* 2016;16: 176-189.

[9] Wong A, Bernath P.F., Rey M., Nikitin A.V., Tyuterev V.G., Atlas of Experimental and Theoretical High-temperature Methane Cross Sections from T=295 to 1000K in the Near-infrared *The*

Astrophysical Journal Supplement Series 2019;240: 4.

[10] Nikitin A.V., Ivanova Y.A., Rey M., Tashkun S.A., Toon G.C., Sung, K., Tyuterev Vl.G., Analysis of PH3 spectra in the Octad range 2733–3660 cm-1 *J. Quant. Spectrosc. Radiat. Transf.* 2017;203: 472-479.

[11] Rey M., Chizhmakova I.S., Nikitin A.V., Tyuterev Vl.G., Understanding global infrared opacity and hot bands of greenhouse molecules with low vibrational modes from first-principles calculations: The case of CF4 *Phys. Chem.Chem. Phys.* 2018;20, no. 32: 21008-21033.

[12] Nikitin A.V., Rey M., Tyuterev Vl.G., First fully ab initio potential energy surface of methane with a spectroscopic accuracy *J. Chem. Phys.* 2016;145: 114309.

[13] Morgan W.J., Matthews D.A., Ringholm M., Agarwal J., Gong J.Z., Ruud K., Allen W.D., Stanton J.F., Schaefer H.F., Geometric Energy Derivatives at the Complete Basis Set Limit: Application to the Equilibrium Structure and Molecular Force Field of Formaldehyde *J. Chem. Theory Comput.* 2018;14: 1333−1350.

[14] Yachmenev A., Yurchenko S.N., Jensen P., Thiel W., A new “spectroscopic” potential energy surface for formaldehyde in its ground electronic state *J. Chem. Phys.* 2011;134: 244307-12.

[15] Burleigh D.C., McCoy A.B., Sibert E.L. III, An accurate quartic force field for formaldehyde *J. Chem. Phys* 1996;104: 480.

[16] Martin, J. M. L.; Lee, T. J., An accurate ab initio Ouartic Force Field for Formaldehyde and its Isotopomers *J. Molec. Spectrosc.* 1993;160: 105-116.

[17] Burleigh D.C. , Sibert E.L., A random matrix approach to rotation-vibration mixing in H2CO and D2CO *J. Chem. Phys.* 1993;98: 8419-8431.

[18] Mladenovic M., Discrete variable approaches to tetratomic molecules Part II: application to H2O2 and H2CO *Spectrochimica Acta Part A* 2002;58: 809-824.

[19] Yagi K., Oyanagi C., Taketsugu T., Hirao K., Ab initio potential energy surface for vibrational state calculations of H2CO *J. Chem. Phys.* 2003;118: 1653-1660.

[20] Al-Refaie A. F., Yachmenev A., Tennyson J., Yurchenko S. N., "ExoMol line lists – VIII. A variationally computed line list for hot formaldehyde," *MNRAS*, vol. 448, pp. 1704-1714, 2015.

[21] Partridge H. , Schwenke D.W., The determination of an accurate isotope dependent potential energy surface for water from extensive ab initio calculations and experimental data *J. Chem. Phys.* 1997;106: 4618-4639.

[22] Polyansky O.L., Zobov N.F., Viti S., Tennyson J, Bernath P.F., Wallace L., Water on the sun:line assignments based on variational calculations. *Science* 1997;277, no. 5324: 346–8.

[23] Tennyson J., Barletta P., Kostin M.A., Polyansky O.L., Zobov N.F., Ab initio rotation–vibration energy levels of triatomics to spectroscopic accuracy *Spectrochimica Acta A* 2002;58, no. 4: 663-672.

[24] Polyansky O., Ovsyannikov R., Kyuberis A., Lodi L., Tennyson J., Zobov N., Calculation of Rotation-Vibration Energy Levels of the Water Molecule with Near-Experimental Accuracy Based on an ab Initio Potential Energy Surface. *J. Phys. Chem. A* 2013;117, no. 39: 9633–9643.

[25] Huang X., Schwenke D.W., Tashkun S.A., al. et, An isotopic-independent highly accurate potential energy surface for CO2 isotopologues and an initial (C16O2)-C-12 infrared line list *J. Chem. Phys.* 2012;136: 124311.

[26] Huang X., Freedman R.S., Tashkun S.A., Schwenke D.W., Lee T.J., Semiempirical 12C16O2 IR line lists for simulations up to 1500K and 20000cm-1. *J.Quant.Spectrosc.Radiat.Transf.* 2013;139: 134–46.

[27] Yurchenko S.N., Barber R.J., Yachmenev A., Thiel W., Jensen P., Tennyson J., A Variationally Computed T = 300 K Line List for NH3 *J. Phys. Chem. A* 2009;113, no. 43: 11845–11855.

[28] Cours T., Rosmus P., Tyuterev V.G., Ab initio dipole moment functions of H232S and intensity anomalies in rovibrational spectra. *J. Chem. Phys.* 2002;117, no. 11: 5192–5208.

[29] Azzam A.A., Lodi L., Yurchenko S.N., Tennyson J., The dipole moment surface for hydrogen sulfide H2S *J.Quant.Spectrosc.Radiat.Transf.* 2015;161: 41-49.

[30] Huang X.C., Schwenke D.W., T.J. Lee, Highly accurate potential energy surface, dipole moment surface, rovibrational energy levels, and infrared line list for (SO2)-S-32-O-16 up to 8000 cm-1 *J. Chem. Phys.* 2014;140, no. 11: 114311.

[31] Tyuterev Vl.G., Kochanov R.V., Tashkun S.A., Holka F., Szalay P.G., New analytical model for the ozone electronic ground state potential surface and accurate ab initio vibrational predictions at high energy range *J. Chem. Phys.* 2013;139: 134307.

[32] Barbe A., Mikhailenko S., Starikova E., al. et, Ozone spectroscopy in the electronic ground state: High-resolution spectra analyses and update of line parameters *J. Quant. Spectrosc. Radiat. Transf.* 2013;130: 172-190.

[33] Tyuterev Vl.G., Kochanov R.V., Campargue A., Kassi S., Mondelain D., Barbe A., Does the "reef structure" at the ozone transition state towards the dissociation exist? New insight from calculations and ultrasensitive spectroscopy experiments *Phys.Rev.Lett* 2014;113: 143002.

[34] Tyuterev V.G., Barbe A., Jacquemart D., Janssen C., Mikhailenko S.N., Starikova E.N., Ab initio predictions and laboratory validation for consistent ozone intensities in the MW, 10 and 5 μ m ranges *J. Chem. Phys.* 2019;150, no. 18: 184303.

[35] Dawes R., Lolur P., Ma J., Guo H., Highly accurate ozone formation potential and implications for kinetics. *J. Chem. Phys.* 2011;135: 081102.

[36] Kokoouline V., Lapierre D., Alijah A., Tyuterev Vl.G., Localized and delocalized bound states of the main isotopologue 48O3 and of 18O-enriched 50O3 isotopomers of the ozone molecule near the dissociation threshold. *Phys. Chem. Chem. Phys.* 2020;22: 15885 - 15899.

[37] Yuen C.H., Lapierre D., Gatti F., Kokoouline V., Tyuterev V.G., The Role of Ozone Vibrational Resonances in the Isotope Exchange Reaction 16O16O+18O→18O16O+16O: The Time-Dependent

Picture *J. Chem. Phys.* 2019;123, no. 36: 7733-7743.

[38] Huang X., Schwenke D.W., Lee T.J., Rovibrational spectra of ammonia. I. Unprecedented accuracy of a potential energy surface used with nonadiabatic corrections *J. Chem. Phys.* 2011;134, no. 4: 044320.

[39] Yurchenko S.N., Carvajal M., Thiel W, Jensen P., Ab initio dipole moment and theoretical rovibrational intensities in the electronic ground state of PH3 *J. Molec. Spectrosc.* 2006;239: 71-87.

[40] Sousa-Silva C., Yurchenko S.N., Tennyson J., A computed room temperature line list for phosphine *J. Molec. Spectrosc.* 2013;288: 28-36.

[41] Nikitin A.V., Rey M., Tyuterev Vl.G, High order dipole moment surfaces of PH3 and ab initio intensity predictions in the Octad range *J. Molec. Spectrosc* 2014;305: 40-47.

[42] Owens A., Yurchenko S.N., Yachmenev A., Tennyson J., Thiel W., Accurate ab initio vibrational energies of methyl chloride *J. Chem. Phys.* 2015;142: 244306.

[43] Owens A., Yurchenko S.N., Yachmenev A., Thiel W., A global potential energy surface and dipole moment surface for silane *J. Chem. Phys.* 2015;143: 244317.

[44] Delahaye T., Nikitin A., Rey M., Szalay P., Tyuterev Vl.G., A new accurate ground-state potential energy surface of ethylene and predictions for rotational and vibrational energy levels *J. Chem. Phys.* 2014;141: 104301.

[45] Delahaye T., Nikitin A.V., Rey M., Szalay P.G., Tyuterev V.G., Accurate 12D dipole moment surfaces of ethylene *Chem. Phys. Letters* 2015;639: 275-282.

[46] Li J., Carter S., Bowman J.M., Dawes R., Xie D., Guo H., High-Level, First-Principles, Full-Dimensional Quantum Calculation of the Ro-vibrational Spectrum of the Simplest Criegee Intermediate (CH2OO) *J. Phys. Chem. Lett.* 2014;5, no. 13: 2364–2369.

[47] Nikitin A.V., Rey M., Chizhmakova I.S., Tyuterev Vl.G., First Full-Dimensional Potential Energy and Dipole Moment Surfaces of SF6 *J. Phys. Chem. A* 2020;124, no. 35: 7014–7023.

[48] Polyansky O., Kyberis A., Zobov N., Tennyson J., Yurchenko S., Lodi L., ExoMol molecular line lists XXX: a complete high-accuracy line list for water *MNRAS* 2018;480, no. 2: 2597-2608.

[49] Lukka T.J., A simple method for the derivation of exact quantum-mechanical vibration-rotation Hamiltonians in terms of internal coordinates *J. Chem. Phys.* 1995;102: 3945.

[50] Colwell S.M. , Handy N.C., The derivation of vibration-rotation kinetic energy operators in internal coordinates. II *Molec. Phys.* 1997;92: 317.

[51] Bramley M.J. , Carrington T.Jr., A general discrete variable method to calculate vibrational energy levels of three- and four-atom molecules *J. Chem. Phys.* 1993;99: 8519-8541.

[52] Poulin N.M., Bramley M.J., Jr. CarringtonT., Kjaergaard H.G., Henry B.R., Calculation of vibrational (J=0) excitation energies and band intensities of formaldehyde using the recursive residue

generation method. *J. Chem. Phys.* 1996;104: 7807-7820.

[53] Makarewicz J. , Skalozub A., Rovibrational Molecular Hamiltonian in Mixed Bond-Angle and Umbrella-Like Coordinates *J. Phys. Chem. A.* 2007;111: 7860-7869.

[54] Nikitin A.V., Holka F., Tyuterev Vl.G., Fremont J., Vibration energy levels of the PH3, PH2D, and PHD2 molecules calculated from high order potential energy surface *J. Chem. Phys* 2009;131: 244312.

[55] Nikitin A.V., Rey M., Tyuterev Vl.G., Rotational and vibrational energy levels of methane calculated from a new potential energy surface *Chem. Phys. Lett.* 2011;501: 179-186.

[56] Werner H.-J., Knowles P.J., Knizia G., Manby F.R., al. et, Molpro: a general purpose quantum chemistry program package *WIREs Comput Mol Sci* 2012;2: 242--253.

[57] Werner H.- J., Knowles P.J, Lindh R., al. et., MOLPRO, version 2019.1, a package of ab initio programs; http://www.molpro.net.

[58] Schwenke D.W. , Partridge H., Vibrational energy levels for CH4 from an ab initio potential *Spectrochim. Acta A* 2001;57: 887.

[59] Brünken S., Müller H.S. P., Lewen F., High accuracy measurements on the ground state rotational spectrum of formaldehyde (H2CO) up to 2 THz. *Phys. Chem. Chem. Phys.* 2003;5: 1515−1518.

[60] Müller H.S. P. , Lewen F., Submillimeter spectroscopy of H2C17O and a revisit of the rotational spectra of H2C18O and H2C16O. *J. Molec. Spectrosc.* 2017;331: 28−33.

[61] Muller H.S.P., Winnewisser G., Demaison J., Perrin A., Valentin A., The Ground State Spectroscopic Constants of Formaldehyde *J. Molec. Spectrosc.* 2000;200: 143-144.

[62] M. Born , Huang K., *Dynamical theory of crystal lattices , Oxford at the Clarendon Press*. Oxford at the Clarendon Press: Clarendon Press, 1954.

[63] Handy N.C., Yamaguchi Y., Schaefer H.F., The diagonal correction to the Born-Oppenheimer approximation: Its effect on the singlet-triplet splitting of CH2 and other molecular effects. *J. Chem. Phys.* 1986;84: 4481–4484.

[64] Cencek W. , Kutzelnigg W., Accurate adiabatic correction for the hydrogen molecule using the Born-Handy formula. *Chem. Phys. Lett.* 1997;266: 383 – 387.

[65] Gauss J., Tajti A., Kállay M., Stanton J.F., Szalay P.G., Analytic calculation of the diagonal Born-Oppenheimer correction within configuration-interaction and coupled-cluster theory. *J. Chem. Phys.* 2006;125: 144111.

[66] Tajti A., Szalay P.G., Gauss J., Perturbative treatement of the electron-correlation contribution to the diagonal Born-Oppenheimer correction. *J. Chem. Phys.* 2007;127: 014102.

[67] Szalay P.G., Holka F., Fremont J., Rey M, Peterson K.A., Tyuterev Vl.G., Are ab initio quantum chemistry methods able to predict vibrational states up to the dissotiation limit for multi-electron

molecules close to spectroscopic accuracy? *Phys. Chem. Chem. Phys.* 2011;13: 3654–3659.

[68] Holka F., Szalay P.G., Fremont J., Rey M., Peterson K.A., Tyuterev Vl.G., Accurate ab initio determination of the adiabatic potential energy function and the Born-Oppenheimer breakdown corrections for the electronic ground state of LiH isotopologues. *J. Chem. Phys.* 2011;134: 094306.

[69] Noga J. , Bartlett R.J., The full CCSDT model for molecular electronic structure. *J. Chem. Phys.* 1987;86: 7041.

[70] Oliphant N. , Adamowicz L., Coupled-cluster method truncated at quadruples. *J. Chem. Phys.* 1991;95: 6645.

[71] Kucharski S.A. , Bartlett R.J., The coupled-cluster single, double, triple, and quadruple excitation method. *J. Chem. Phys.* 1992;97: 4282.

[72] Bomble Y.J., Stanton J.F., Kállay M., Gauss J., Coupled cluster methods including noniterative corrections for quadruple excitations. *J. Chem. Phys.* 2005;123: 054101.

[73] Matthews D.A. , Stanton J.F., Non-orthogonal spin-adaptation of coupled cluster methods: A new implementation of methods including quadruple excitations *J. Chem. Phys.* 2015;142: 064108.

[74] Matthews D.A. , Stanton J.F., Accelerating the convergence of higher-order coupled cluster methods. *J. Chem. Phys. 2015, 143, 204103* 2015;143: 204103.

[75] Owens A., Yurchenko S.N., Yachmenev A., Tennyson J., Thiel W., A highly accurate ab initio potential energy surface for methane *J. Chem. Phys.* 2016;145: 104305.

[76] Stanton J.F., Gauss J., Harding M.E., Szalay P.G., al. et. CFour program http://www.cfour.de.

[77] Perez R., Brown J.M., Utkin Y., Han J., Curl R.F., Observation of hot bands in the infrared spectrum of H2CO *J. Molec. Spectrosc.* 2006;236: 151-157.

[78] Perrin A., Valentin A., Daumont L., New analysis of the 2v4, v4+v6, 2v6, v3+v4, v3+v6, v1, v5, v2+v4, 2n3, v2+v6 and v2+v3 bands of formaldehyde H2 12C16O: Line positions and intensities in the 3.5 mm spectral region *Journal of molecular structure* 2006;780–781: 28-44.

[79] Flaud J., Lafferty W., Sams R., Sharpe S., High resolution spectroscopy of H2 12C16O in the 1.9 to 2.56 µm spectral range *Molec. Phys.* 2006;104: 1891.

[80] Bouwens R.J., Hammerschmidt J.A., Grzeskowiak M.M., Stegink T.A., Yorba P.M., Polik W.F., Pure vibrational spectroscopy of S 0 formaldehyde by dispersed fluorescence *J. Chem. Phys.* 1996;104: 460.

[81] Perrin A., Keller F., Flaud J.-M., New analysis of the v2, v3, v4, and v6 bands of formaldehyde H2 12C16O line positions and intensities in the 5–10 lm spectral region *J. Molec. Spectrosc.* 2003;221: 192-198.

[82] Perrin A., Flaud J.-M., Predoi-Cross A., Winnewisser M., Winnewisser B.P., Mellau G., Lock M., New High-Resolution Analysis of the v3 , v4 , and v6 Bands of D2CO Measured by Fourier Transform

Spectroscopy *J. Molec. Spectrosc.* 1998;187: 61-69.

[83] Rey M., Group-theoretical formulation of an Eckart-frame kinetic energy operator in curvilinear coordinates for polyatomic molecules *J. Chem. Phys.* 2019;151: 024101.

[84] Rey M., Nikitin A.V., Tyuterev V.G., Complete nuclear motion Hamiltonian in the irreducible normal mode tensor operator formalism for the methane molecule *J. Chem. Phys* 2012;136, no. 24: 244106.

[85] Rey M., Nikitin A.V., Tyuterev Vl.G., First principles intensity calculations of the methane rovibrational spectra in the infrared up to 9300 cm-1. *Phys. Chem.Chem. Phys.* 2013;15, no. 25: 10049-10061.

[86] Rey M., Nikitin A.V., Tyuterev Vl.G., Convergence of normal mode variational calculations of methane spectra: Theoretical line list in the icosad range computed from potential energy and dipole moment surfaces *J. Quant. Spectrosc. Radiat. Transfer.* 2015;164: 207–220.

[87] Lohilahti J. , Alanko S., The v2 Band of Formaldehyde-d2 *J. Molec. Spectrosc.* 2001;205: 248-251.

[88] Lohilahti J., Ulenikov O.N., Bekhtereva E.S., Alanko S., Anttila R., High resolution infrared study of D2CO in the region of 1780–2400 cm-1: assignment and preliminary analysis *J.Molec. Structure* 2006;780-781: 182-205.

[89] Tyuterev Vl.G., Tashkun S.A., Rey M., Kochanov R.V., Nikitin A.V., Delahaye T., Accurate spectroscopic models for methane polyads derived from a potential energy surface using high-order contact transformations. *J.Phys.Chem. A* 2013;117: 13779-13805.

[90] Nikitin A.V., Thomas X., Daumont L., Rey M., Sung K., Toon G.C., Smith M.A.H., Mantz ProtasevichA.E., A.W., Tashkun S.A., Tyuterev Vl.G., Assignment and modelling of 12CH4 spectra in the 5550–5695, 5718–5725 and 5792–5814 cm−1 regions *J. Quant. Spectrosc. Radiat. Transfer* 2018;219: 323–332.

[91] Nikitin A.V., Protasevich A.E., Rey M., Tyuterev V.G., Highly excited vibrational levels of methane up to 10 300 cm−1: Comparative study of variational methods *J. Chem. Phys.* 2018;149: 124305.

582